THE EFFECTS OF VIBRATION ON AN INERTIAL MEASUREMENT UNIT

Thesis For The Degree Of M.S. MICHIGAN STATE UNIVERSITY

LOUIS RALPH PAPALE
1966

THESIS

LIBRARY
Michigan State
University

THE EFFECTS OF VIBRATION ON AN INERTIAL MEASUREMENT UNIT

Louis Ralph Papale

AN ABSTRACT

Submitted to
Michigan State University
in partial fulfillment of the requirements
for the degree of

MASTER OF SCIENCE

Department of Electrical Engineering

1966

ABSTRACT

THE EFFECTS OF VIBRATION
ON AN
INERTIAL MEASUREMENT UNIT

By Louis Ralph Papale

In this thesis, the errors produced by both sinusoidal and random vibration acting on an inertial measurement unit are considered. The sources of vibration in missiles are presented and the vibration characteristics are established. A brief description of an inertial measurement unit and its major components, which consist of the gimbal system, the accelerometers and the gyros, are presented. A state model of the gimbal system is developed and an example of the state model to the design of an inertial measurement unit is presented. The particular design considerations associated with vibration are indicated. Analyses of the accelerometers and the gyros are performed. The error equations for the vibropendulous error, the nonlinearity error and the scale factor error of a pendulous, pulse-rebalance accelerometer are derived. The error equation is developed for the anisoelastic effects of a gyro under sinusoidal vibration. The system error equations are derived for both the sinusoidal and random vibration effects on an inertial measurement unit. The significance of the vibration effects are illustrated and means for minimizing the effects are indicated.

THE EFFECTS OF VIBRATION ON AN INERTIAL MEASUREMENT UNIT

Louis Ralph Papale

A THESIS

Submitted to
Michigan State University
in partial fulfillment of the requirements
for the degree of

MASTER OF SCIENCE

Department of Electrical Engineering

1966

R. K. J. K.

"The aim of science is to seek the simplest explanation of complex facts. We are apt to fall into the error of thinking that the facts are simple because simplicity is the goal of our quests. The guiding model in the life of every natural philosopher should be 'Seek simplicity and distrust it'."

by Alfred North Whitehead "Concepts of Nature"

ACKNOWLEDGEMENTS

I wish to extend my graditude to several persons who so willingly provided assistance during the preparation of this thesis. Special thanks go to my advisor, Dr. H. Hedges of the MSU Electrical Engineering Department, for reviewing the material and offering many helpful suggestions. My graditude goes to Dr. R. Dubes, also of the MSU Electrical Engineering Department, who reviewed the portion on random vibration and provided many improvements. I would also like to thank Mrs. Ann La Comte for typing the manuscript, and LSI Publications Department for its publication. Finally, a "thank you" to my wife Jo for her admirable patience throughout the preparation of this thesis.

TABLE OF CONTENTS

																Page
LIST	OF I	LUSTRATIO	DNS											•		v
1.0	INTRO	DUCTION .												•		1
2.0	SOUR	CES OF VI	BRATION										•		•	5
3.0	DESC	RIPTION OF	AN INE	RTIAL	MEAS	UREN	MENT	UNI	T		•		•		•	14
4.0	STATI	MODEL OF	A STAB	LE PLA	ATFOR	em .										18
5.0	AN AI	PLICATION	OF THE	PLATE	FORM	STAT	ГЕ М	ODEL	•	•		•	•	•	•	25
	5.1	Terminal	Equatio	n Para	mete	rs			•		•	•	•		•	25
	5.2	Solution	of the	State	Mode	1					•	•	•	•	•	31
	5.3	Design Co	onsidera	tions	•				•	•		•	•		•	3 6
6.0	EFFE	CT OF SINU	JSOIDAL	VIBRAT	ΓION	ON I	PLAT	FORM	II.	IST	'RU	ME	NT	`S	•	3 9
	6.1	Acceleron	neters						•					•	•	39
		6.1.1 Vi	.bropend	ulous	Erro	rs										42
		6.1.2 No	nlinear	ities											•	49
		6.1.3 So	cale Fac	tor E	ror									•	•	51
	6.2	Gyros .							•		•				•	53
		6.2.1 Ma	ıs s Unba	lance	Drif	it .							•		•	54
		6.2.2 Ar	nisoelas	tic Dı	rift				•	•		•	•	•	•	56
7.0	SYSTI	EM ERROR I	OUE TO S	INUSO	DAL	VIBI	RATI	ON .				•			•	59
8.0	EFFE	CT OF RANI	OM VIBR	ATION	ON P	LATI	FORM	INS	TRU	ME	NT	`S	•	•	•	68
	8.1	Acceleron	neters						•		•	•	•	•	•	68
		8.1.1 Vi	bropend	ulous	Erro	r.						•	•		•	68
		8.1.2 No	nlinear	ities												78

TABLE OF CONTENTS (cont)

																			Page
		8.1.3	Scale	e Fact	tor E	rro	r.		•			•		•	•	•	•		81
	8.2	Gyros		• •		•			•	•		•					•	•	86
		8.2.1	Mass	Unba	lance	Dr	ift	•	•			•			•	•	•	•	8 6
		8.2.2	Anis	oelasi	tic [rif	t.	•		•			•		•	•	•	•	88
9.0	SYST	EM ERRO	R DUE	TO R	ANDOM	ı VI	BRA	TI	ON	•	•	•			•		•	•	91
10.0	CONC	LUSIONS		• •				•				•						•	99
	Refe	rences				_		_		_					_	_			100

LIST OF ILLUSTRATIONS

Figure			Page
1	High Speed Rocket Sled		6
2	Mean Power Level Measured on a Rocket Sled		7
3	Power Spectral Density Measured on a Rocket Sled 8 Seconds After First Motion	•	8
4	Power Spectral Density Measured on a Rocket Sled 14 Seconds After First Motion	•	9
5	Noise Levels for Boost Flight		12
6	Generalized System Block Diagram	•	16
7	Two Types of IMU		17
8	IMU Gimbal System		20
9	A Typical IMU		21
10	Axial Deflection vs. Axial Load for a Single Bearing	•	29
11	Radial Deflection vs. Radial Load for a Single Bearing	•	30
12	Platform - Theoretical Vibratory Response		37
13	Pendulous Force - Balance Accelerometer with Analog Output	•	40
14	Pendulous Force - Balance Accelerometer with Pulse Output	•	45
15	System Error Model		60
16	Contribution to System Error by Platform Instruments Due to Sinusoidal Vibration	•	66
17	Effect of Accelerometer Scale Factor Error on Signal Distribution	•	82
18	Contribution to System Error by Platform Instruments Due to Random Vibration	•	98

1.0 INTRODUCTION

The major part of the missile target error produced by an inertial guidance system is, in general, caused by instrument imperfections. However, a significant consideration, from the standpoint of both the error contribution and the design, is the effect of vibration on the instruments. This thesis considers the effects of vibration on the instruments as utilized in an inertial measurement unit from the standpoint of accuracy and design considerations.

The errors in an inertial guidance system can be allocated to four major groups:

- 1. Instrument imperfections.
- 2. Initial alignment.
- 3. Simplification of guidance equations.
- 4. Vibration.

The first two are generally included in the error analyses considered for each system. The third is evaluated when establishing the guidance equations and should represent a small error relative to the first two error sources. The fourth error source may be a significant amount depending on the characteristics of the instruments and the vibration environment. It is imperative in the design of an inertial measurement unit to establish the errors arising from vibration. Such a determination provides the means of selection of the type of instruments to be used, such as floated

or non-floated gyros; it is important from the standpoint of reliability as well as for establishing the need for vibration isolation.

In the development of inertial measurement units, the usual shock and vibration tests are performed in the laboratory to establish the functional capability of the system. A more elaborate test prior to actual flight test is to subject the IMU to a high speed sled test environment. This allows the unit to be tested in an environment much like that of a missile.

The material herein, although quite general with respect to inertial measurement units, presents an example of the development of a specific type of an IMU. This development program was carried to a point beyond the normal laboratory testing phase and included a high speed sled test program at Holloman Air Force Base, New Mexico. Examples of actual data obtained at the track are included.

Specifically, the material herein presents a unified treatment of the effects of vibration on an IMU from the standpoint of both sinusoidal and random vibration. The particular points of accomplishment are as follows:

- 1. A state model of the IMU gimbal system is derived.
- An example of the application of the state model to a specific IMU is presented, and the design considerations for future engineering efforts are outlined.

- The error equations for the vibropendulous error of a pulse-rebalance accelerometer are derived.
- 4. The error equations for the nonlinearity errors for an accelerometer are developed.
- 5. The error equations for the scale factor error of a pulse-rebalance accelerometer are derived.
- 6. The error equation for the anisoelastic effects of a gyro under sinusoidal vibration is developed.
- 7. The system error equations for both the sinusoidal and random vibration effects on an IMU are derived.

In summary, the contribution of vibration to the IMU system error can be significant, and can range to as high as 25% of the allowable miss distance, depending on the level of vibration. The particular features to be considered in minimizing the vibration effects are pointed out.

The arrangement of the material is based upon the logical flow of the vibration from the missile structure to the platform instruments. Consequently, the first consideration is the missile environment and the characteristics of vibration. This, then, describes the input signal at the case of the IMU. Following this

discussion is a brief description of the IMU and the major items considered in the study which were the gimbal system, the accelerometers, and the gyros. Continuing with the signal flow, the next presentation is the development of the state model of the IMU gimbal system. It is the gimbal system that shapes the environment seen by the platform instruments and is illustrated by an example. The specific error equations for the platform instruments (accelerometers and gyros) due to sinusoidal vibration are developed, and the system error equation due to sinusoidal vibration is formulated. Similarly, the error equations for the platform instruments due to random vibration are derived, and finally, the system error equation for random vibration is developed.

2.0 SOURCES OF VIBRATIONS

Prior to any considerations of the effects of vibrations, it is helpful to review the sources of vibrations in missiles. This section presents a discussion of the three main sources of vibrations in missiles and points out the various characteristics of the vibration which most likely represent the environment of the IMU.

Vibrations in missiles are generated by three main sources:

- 1. The missile power plant.
- 2. Aerodynamic effects, such as boundry layer and turbulence.
- 3. Internal operating components.

In addition to these sources, a high speed sled used in testing inertial guidance systems has one additional vibration source. This is the effect of the slipper and slipper suspension on the track (see Figure 1). Examples of the vibration presented on a rocket sled are shown in Figures 2, 3, and 4.

The missile power plant may consist of a single rocket or a cluster of rockets, depending on the vehicle. All rocket thrust chambers vibrate with variations depending upon the design. The physical mechanism of all these vibrations is not clearly established but basic types of vibrations have been observed in various rocket thrust chamber assemblies. The first is believed to be a

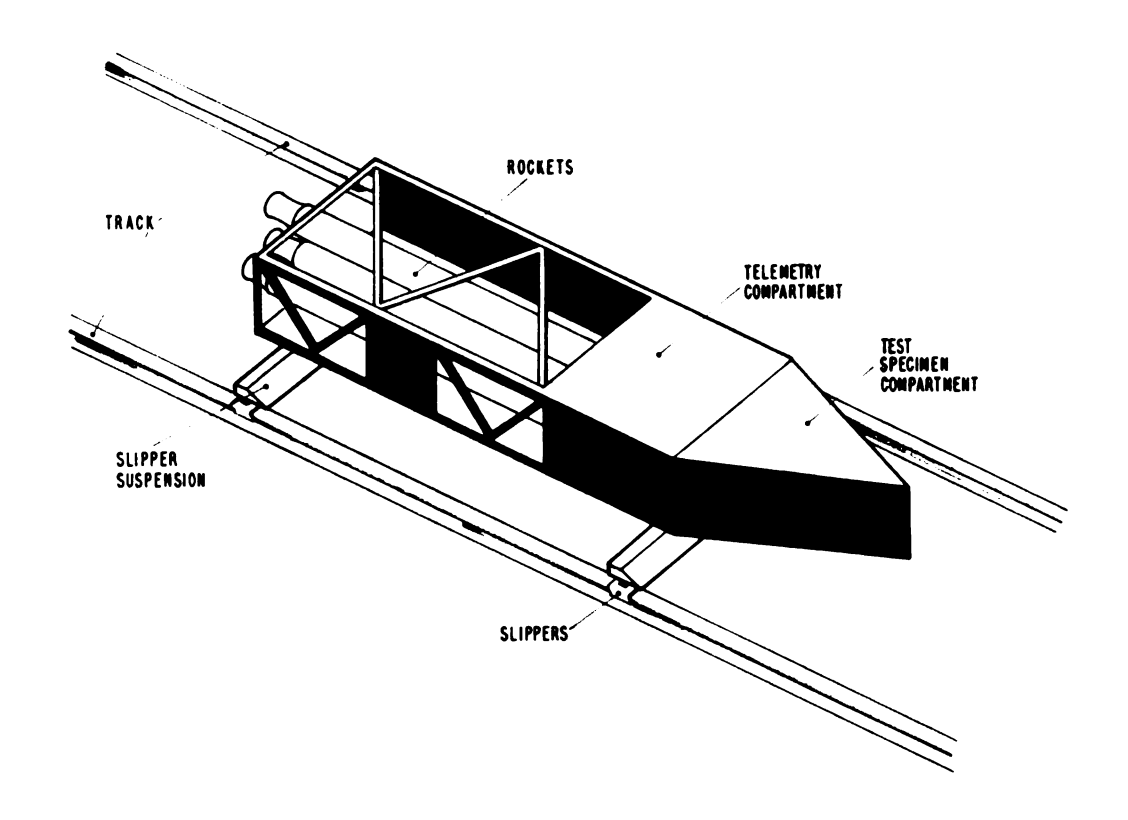
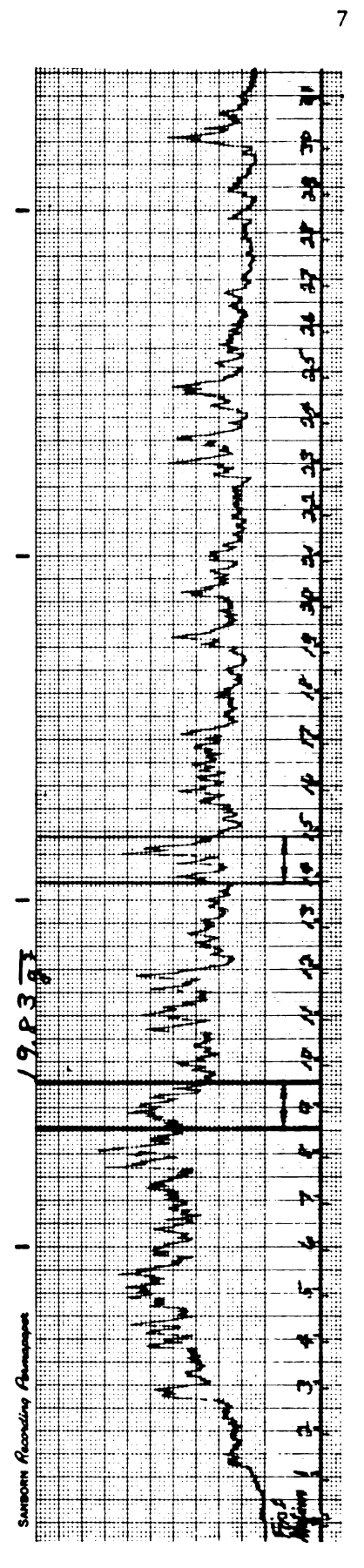


FIGURE 1
HIGH SPEED ROCKET SLED

SAMBORN POWER VS TIME TH

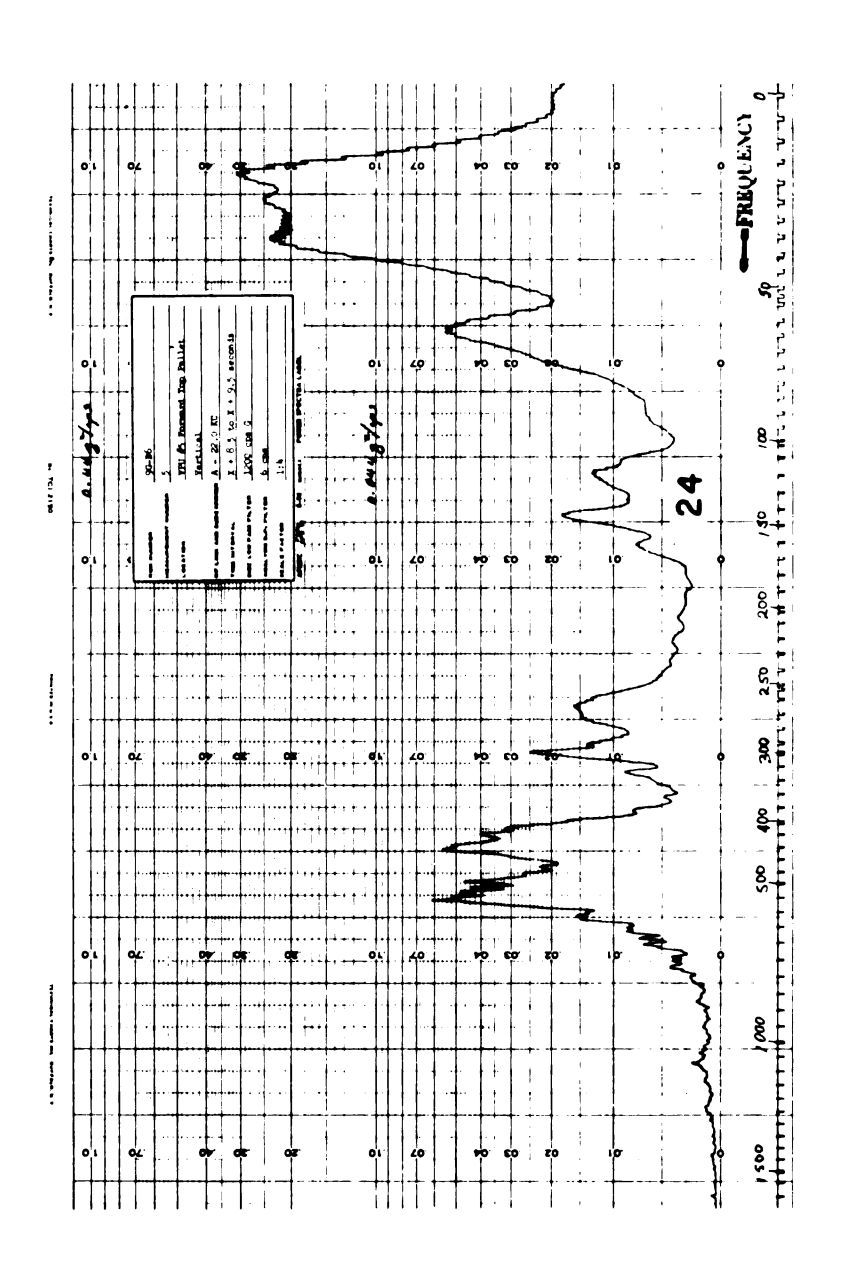


POWER VS TIME

	MOTE: Davies power spectral	intervals. RUN NO. 9G-B6
8	cps G	
22.0 15	1200 cps G	۲
RF Link A-2	Low Pass Filter	Messurement Mo.

FIGURE 2

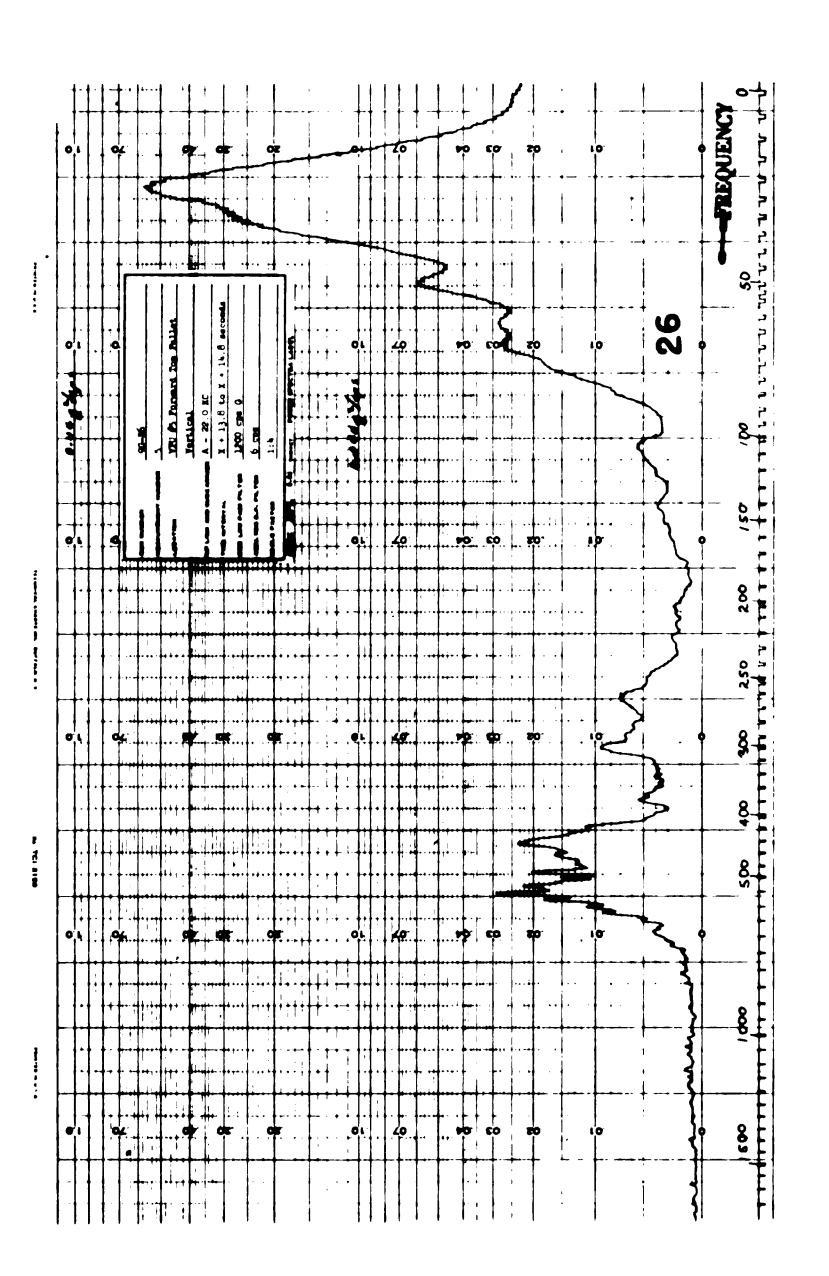
MEAN POWER LEVEL MEASURED ON A ROCKET SLED



POWER SPECTRAL DENSITY MEASURED ON A ROCKET SLED

8 SECONDS AFTER FIRST MOTION

FIGURE 3



POWER SPECTRAL DENSITY MEASURED ON A ROCKET SLED
14 SECONDS AFTER MOTION

FIGURE 4

chamber pressure and feed system oscillation with relatively low frequencies in the range of 0.1 cps to 15 cps. The second type of vibration is that caused by the excitation of the natural frequency of the metal parts, such as the chamber, pipelines, and structural parts. This frequency is usually below 100 cps. The third type is a high pitch, high energy vibration and is associated with the combustion. Overall, the vibration spectrum is of a random nature with the power levels concentrated at the points indicated.

In considering the aerodynamic effects, it can be shown^{7*} that the vibrations due to the boundary layer are caused by surface pressure fluctuations created by turbulence within the boundary layer. In addition, atmospheric turbulence may cause surface pressure fluctuations. Further considerations of aerodynamic effects must take into account the flight conditions (dynamic pressure). These are the vibration conditions that exist in the subsonic state. However, in the transonic region, a condition known as transonic buffeting takes place. This is created by a highly turbulent condition with a build-up of dynamic pressure. One kind of buffet is identified by a white distribution of power in the power spectrum. The transonic region is of major concern because of possible structural and equipment damage. However, the duration of flight through this region is relatively short for missile flights.

^{*} Superscripts refer to the references.

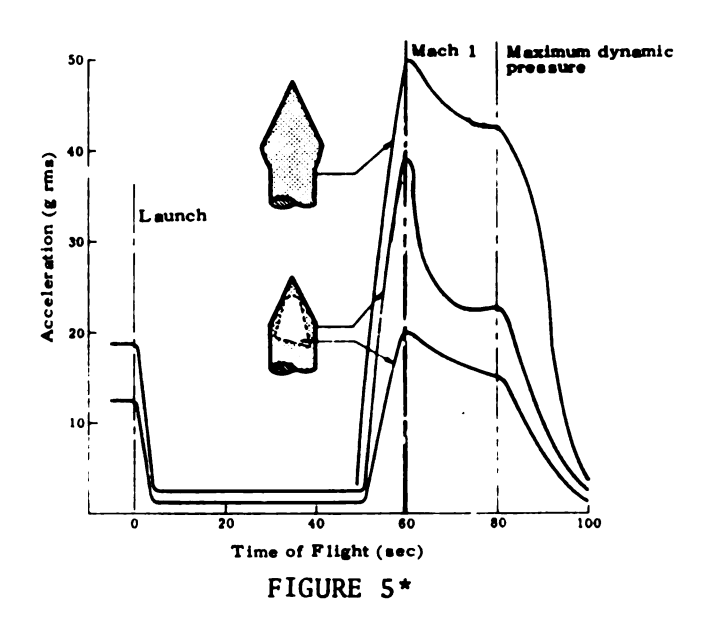
Another kind of buffeting - depending upon the re-entrant angles - is that which takes place due to the detachment of the air flow on bulbous configurations. The pressure fluctuations act over a greater area than the first type of buffet and the frequency distribution of the pressure fluctuations is concentrated more at the low end of the spectrum. The greater the magnitude of this buffeting, the greater the intensity of the lower frequency components which in turn tend to excite the primary structural modes of the vehicle.

Finally, such things as hypersonic buzz (a hinge moment oscillation produced by high speed flight) and flap flutter also lead to vibration effects.

The third item considered as a primary source of vibration is the internal operational components. These, of course, could be such items as motors, hydraulic pumps, inverters, blowers and the like.

It has been shown, in missile experience, that the vibration environment for the vehicle arises principally from acoustic pressures impinging on the vehicle surface. A typical curve of rms acceleration at some location on the re-entry vehicle, e.g., the guidance truss, as a function of flight time is given in Figure 5. At launch, the sound field from the booster engines envelops the re-entry vehicle and excites the structure and its contents. As the

vehicle clears the pad and begins to accelerate, the noise level drops until the excitation is due mostly to thrust pulsations being fed through the structure. As Mach 1 is approached, the buffeting forces build up and the vibration levels exceed those at launch. After Mach 1, the dynamic pressure continues to increase but the flow is less disturbed so that, in general, an intensity plateau is maintained until after maximum dynamic pressure is reached. As the dynamic pressure decreases and the vehicle leaves the atmosphere, the noise again drops to the structural-path contribution level.



NOISE LEVELS FOR BOOST FLIGHT

In producing such vehicles, the design provision for reduction of equipment vibration level utilizes a well-tested procedure for frequency separation called the octave rule. The octave

^{*} Reprinted from "Astronautics and Aerospace Engineering" with permission. 7

rule requires the basic frequency of each component to be an octave higher than that of the structure on which it is mounted. In this way, the possibility of the resonant frequency of one equipment being the same as that of another is avoided.

A typical vibration environment for an inertial measurement unit for a missile is a power spectral density of $0.07g^2/cps$ over a frequency range of 20 to 2000 cps. From a system standpoint, this is a white noise input to the IMU, which is briefly described in the next section.

3.0 DESCRIPTION OF AN INERTIAL MEASUREMENT UNIT

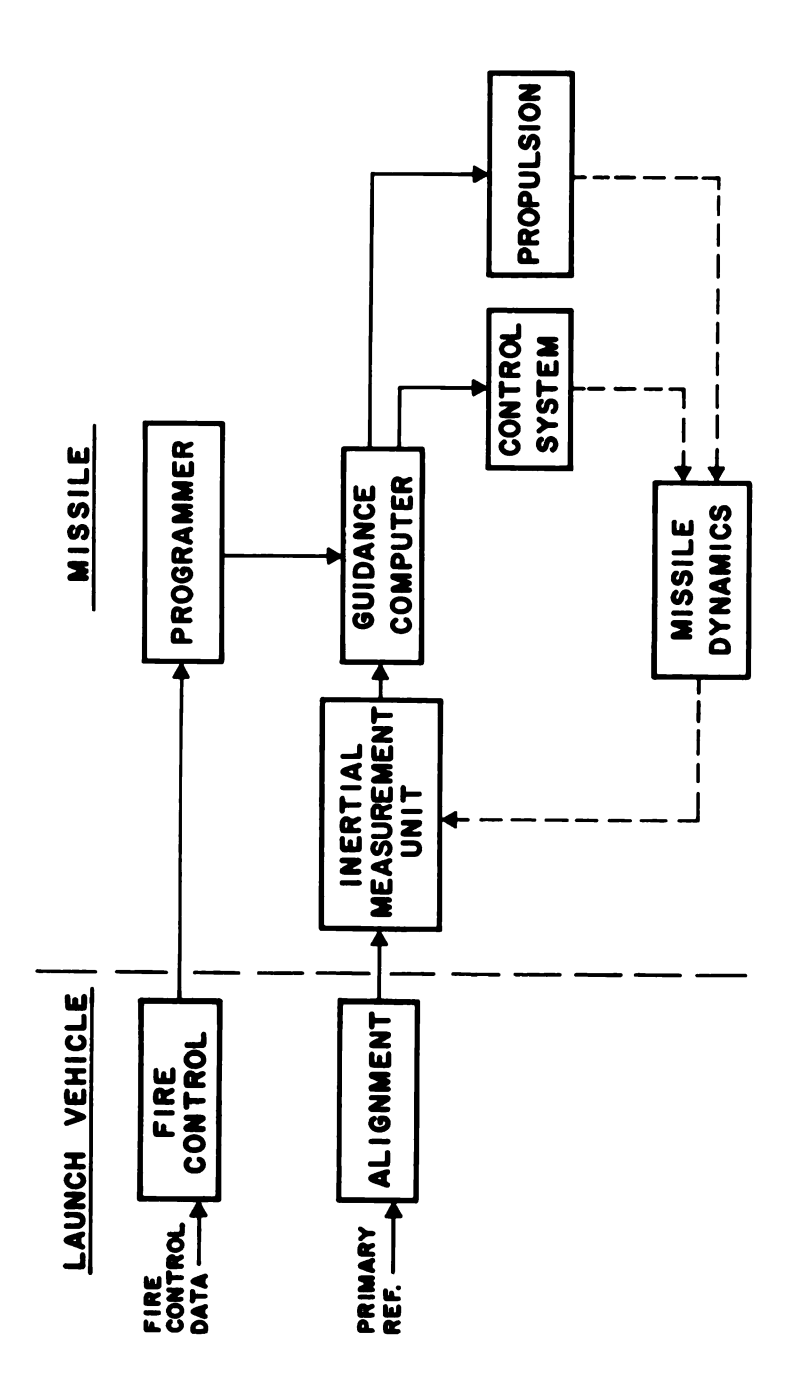
Having established the vibration environment, it is appropriate to consider the IMU per se. This section presents a brief description of an IMU, its function in relation to the missile, and the major components.

An inertial measurement unit is a device capable of measuring any changes in rotational or translational motion with respect to an inertial frame of reference. As implied, the means of operation is based upon Newton's laws of motion and consequently an inertial guidance system is sometimes referred to as a "self-contained system."

From the basics of kinematics it is known that the trajectory of a body may be defined by an appropriate combination of translational and rotational measurements. Thus, to describe the path of a missile, an inertial measurement unit is used to provide such information (see Figure 6). This information is then supplied to a guidance computer in which it is utilized as the present position of the missile. Stored in the guidance computer is a specific program indicating where the missile should be at a particular time. The two pieces of information are compared and the difference then serves as the basis for applying corrections to the propulsion system and/or the control system. Hence, the accuracy of the trajectory is primarily dependent upon the accuracy of the inertial measurement unit.

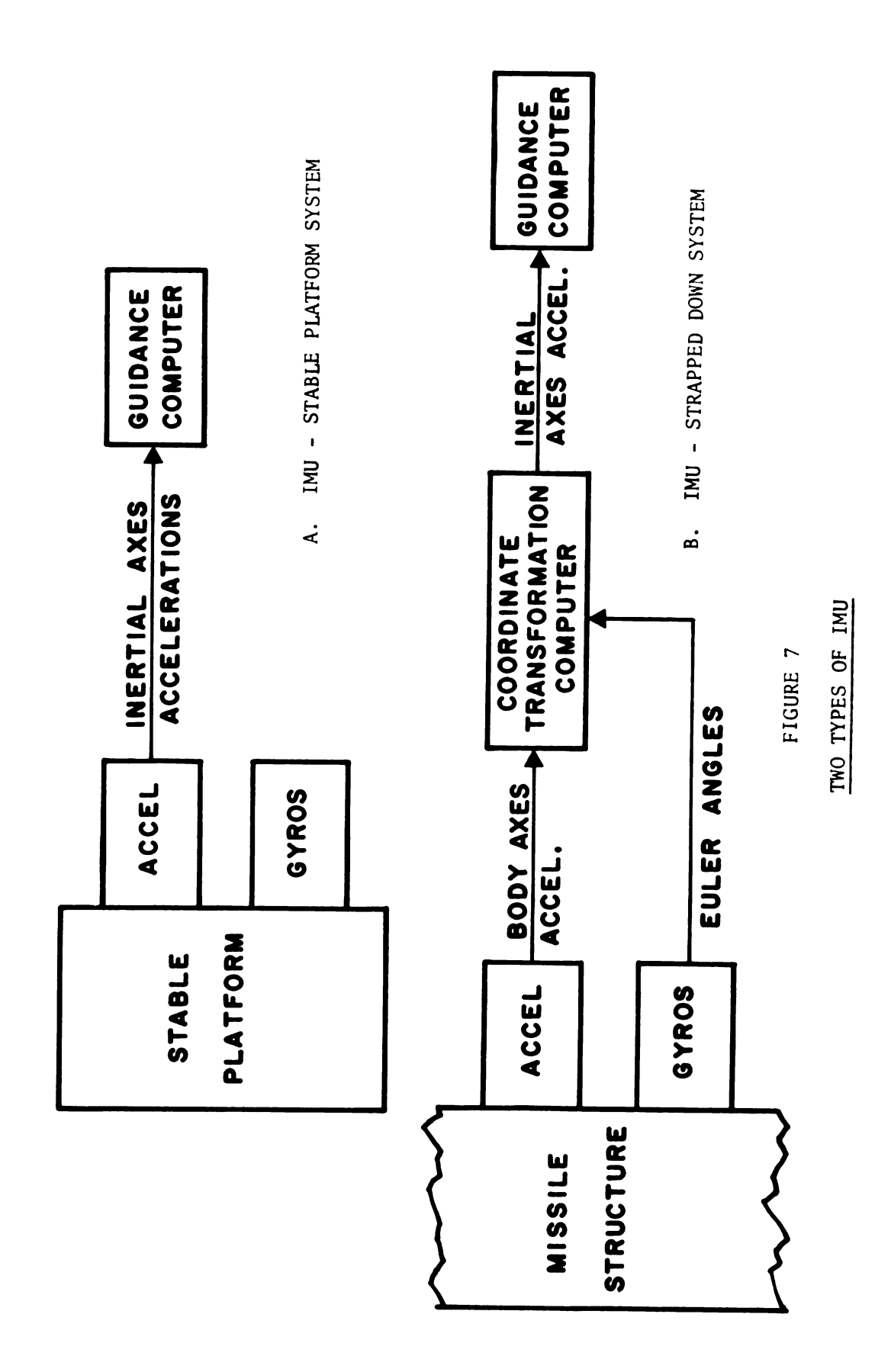
The function of an IMU can be provided in two ways. In either case the basis of operation is the gyro and the accelerometer. One method, known as the stable platform approach, has a mechanical gimbal system which operates as part of a stabilization loop to maintain the accelerometers (located on the stable element) fixed to some reference (see Figure 7A). The second method, known as a strapped-down system, has the accelerometer and gyros located directly on the missile airframe. Hence, a computer is required to convert from the missile body coordinate system to an inertial coordinate system (see Figure 7B).

Consequently, in examining the effects of vibration on an inertial measurement unit, the gyros, accelerometers and the gimbal system must be analyzed. The first thing to be analyzed is the gimbal system which is treated in the next two sections.



GENERALIZED SYSTEM BLOCK DIAGRAM

FIGURE 6



4.0 STATE MODEL OF A GIMBAL SYSTEM

In establishing the effects of vibration on an inertial measurement unit, it is first necessary to develop a methematical model of the gimbal system. This model may then be utilized with specific vibrations present at the missile airframe as described in Section 2.0 to determine the type of vibration seen by the IMU instruments located on the stable platform.

A schematic diagram of a gimbal system can be represented by a combination of spring, mass and damper elements as shown in Figure 8. Three degrees of freedom are indicated since the gimbal system is assumed to consist of three gimbals. Additional degrees of freedom are sometimes introduced in the form of a fourth gimbal or a vibration isolator. However, this is a design parameter and only a slight modification of the state model is required to provide for this.

The analysis herein considers translational motion only since the platform is assumed to be independent of rotations. This is a realistic assumption since the stabilization loops have a capability of maintaining the rotation to a few arc-seconds of motion.

In the mechanical system, each mass element represents the total lumped mass parameter of each gimbal and the particular instruments located on that gimbal. The spring element represents the

stiffness coefficient of the combination of the particular gimbal and the bearings used in the mechanization. The damper element represents the structural damping and windage effects. Figure 9 illustrates a typical IMU with roll, yaw, and pitch gimbals.

The development of the state model for the gimbal system will now be considered.

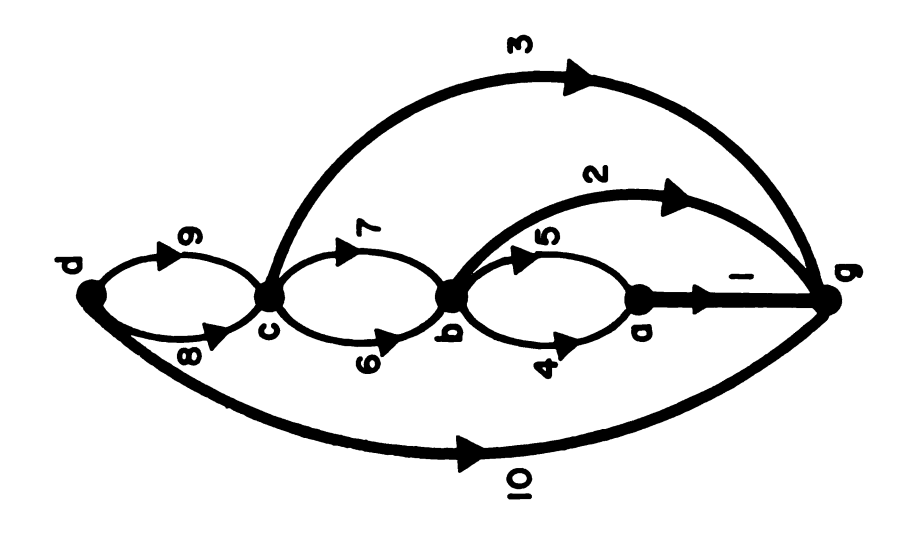
The terminal equations for the components in the system can be written in the form

$$\frac{d}{dt} \begin{bmatrix} \dot{\delta}_{1}(t) \\ \dot{\delta}_{2}(t) \\ \dot{\delta}_{3}(t) \end{bmatrix} = \begin{bmatrix} \frac{1}{M_{1}} & 0 & 0 \\ 0 & \frac{1}{M_{2}} & 0 \\ 0 & 0 & \frac{1}{M_{3}} \end{bmatrix} \begin{bmatrix} f_{1}(t) \\ f_{2}(t) \\ f_{3}(t) \end{bmatrix}$$

$$\frac{d}{dt} \begin{bmatrix} f_{4}(t) \\ f_{6}(t) \\ f_{8}(t) \end{bmatrix} = \begin{bmatrix} K_{4} & 0 & 0 \\ 0 & K_{6} & 0 \\ 0 & 0 & K_{8} \end{bmatrix} \begin{bmatrix} \dot{\delta}_{4}(t) \\ \dot{\delta}_{6}(t) \\ \dot{\delta}_{8}(t) \end{bmatrix}$$

$$\begin{bmatrix} f_{5}(t) \\ f_{7}(t) \\ f_{9}(t) \end{bmatrix} = \begin{bmatrix} D_{5} & 0 & 0 \\ 0 & D_{7} & 0 \\ 0 & 0 & D_{9} \end{bmatrix} \begin{bmatrix} \dot{\delta}_{5}(t) \\ \dot{\delta}_{7}(t) \\ \dot{\delta}_{9}(t) \end{bmatrix}$$

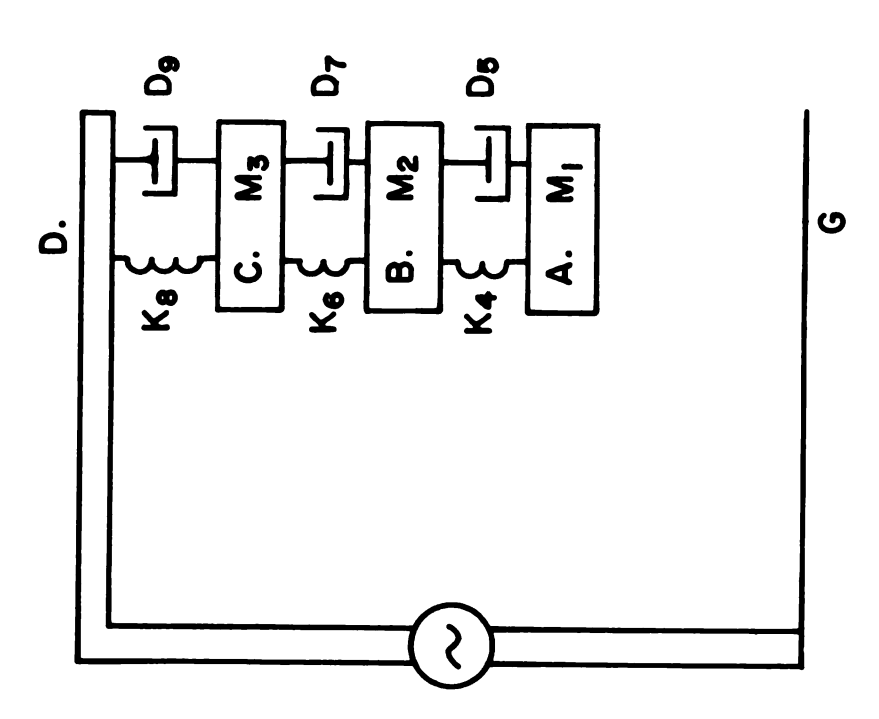
 $\delta_{10}(t)$ a specified across driver



b) SYSTEM GRAPH

FIGURE 8

IMU GIMBAL SYSTEM



a) MECHANICAL SYSTEM

Note that the terminal equations for the mass elements are explicit in the across variables, while the terminal equations for the spring and damper elements are explicit in the through variables. The tree is selected to include elements 1, 2, 3, and the across driver. The normal-form model is developed by first eliminating all tree through variables and all chord across variables in the above terminal equations.

The cutset equations for the through variables yield

$$\begin{bmatrix} f_1 \\ f_2 \\ f_3 \end{bmatrix} = \begin{bmatrix} 1 & 1 & 0 & 0 & 0 & 0 \\ -1 & -1 & 1 & 1 & 0 & 0 \\ 0 & 0 & -1 & -1 & 1 & 1 \end{bmatrix} \begin{bmatrix} f_4 \\ f_5 \\ f_6 \\ f_7 \\ f_8 \\ f_9 \end{bmatrix}$$

Substituting these equations into the terminal equation yields

$$\frac{d}{dt} \begin{bmatrix} \dot{\delta}_{1}(t) \\ \dot{\delta}_{2}(t) \\ \dot{\delta}_{3}(t) \end{bmatrix} = \begin{bmatrix} \frac{1}{M_{1}} & 0 & 0 \\ \frac{-1}{M_{2}} & \frac{1}{M_{2}} & 0 \\ 0 & \frac{-1}{M_{3}} & \frac{1}{M_{3}} \end{bmatrix} \begin{bmatrix} f_{4} \\ f_{6} \\ f_{8} \end{bmatrix} + \begin{bmatrix} \frac{1}{M_{1}} & 0 & 0 \\ \frac{-1}{M_{2}} & \frac{1}{M_{2}} & 0 \\ 0 & \frac{-1}{M_{3}} & \frac{1}{M_{3}} \end{bmatrix} \begin{bmatrix} f_{5} \\ f_{7} \\ f_{9} \end{bmatrix}$$

From the circuit equations the following equations for the across variables may be found

$$\begin{bmatrix} \dot{\delta}_{4}(t) \\ \dot{\delta}_{6}(t) \\ \dot{\delta}_{8}(t) \end{bmatrix} = \begin{bmatrix} 0 & -1 & 1 & 0 \\ 0 & 0 & -1 & 1 \\ 1 & 0 & 0 & -1 \end{bmatrix} \begin{bmatrix} \dot{\delta}_{10} \\ \dot{\delta}_{1} \\ \dot{\delta}_{2} \\ \dot{\delta}_{3} \end{bmatrix}$$

Substituting these equations into the terminal equation gives

$$\frac{d}{dt} \begin{bmatrix} f_{i_1} \\ f_6 \\ f_{\theta} \end{bmatrix} = \begin{bmatrix} -\kappa_{i_1} & \kappa_{i_1} & 0 \\ 0 & -\kappa_6 & \kappa_6 \\ 0 & 0 & -\kappa_8 \end{bmatrix} \begin{bmatrix} \delta_1 \\ \delta_2 \\ \delta_3 \end{bmatrix} + \begin{bmatrix} 0 \\ 0 \\ \kappa_{\theta} \end{bmatrix}$$

From the circuit equations we also have

$$\begin{bmatrix} \dot{\delta}_{5} \\ \dot{\delta}_{7} \\ \dot{\delta}_{9} \end{bmatrix} = \begin{bmatrix} 0 & -1 & 1 & 0 \\ 0 & 0 & -1 & 1 \\ 1 & 0 & 0 & -1 \end{bmatrix} \begin{bmatrix} \dot{\delta}_{10} \\ \dot{\delta}_{1} \\ \dot{\delta}_{2} \\ \dot{\delta}_{3} \end{bmatrix}$$

And substituting these results into the terminal equations gives

$$\begin{bmatrix} \mathbf{f}_5 \\ \mathbf{f}_7 \\ \mathbf{f}_9 \end{bmatrix} = \begin{bmatrix} 0 & -D_5 & D_5 & 0 \\ 0 & 0 & -D_7 & D_7 \\ D_9 & 0 & 0 & -D \end{bmatrix} \begin{bmatrix} \dot{\delta}_{10} \\ \dot{\delta}_{1} \\ \dot{\delta}_{2} \\ \dot{\delta}_{3} \end{bmatrix}$$

Combining the previous equations appropriately yields the state model for the gimbal system as

$$\frac{d}{d\tau} \begin{bmatrix} \delta_{1}(\tau) \\ \delta_{2}(\tau) \\ \delta_{3}(\tau) \\ f_{4}(\tau) \end{bmatrix} = \begin{bmatrix} \frac{-D_{5}}{M_{1}} & \frac{D_{5}}{M_{1}} & 0 & \frac{1}{M_{1}} & 0 & 0 \\ \frac{D_{5}}{M_{2}} & \frac{(-D_{5}+D_{7})}{M_{2}} & \frac{D_{7}}{M_{2}} & \frac{-1}{M_{2}} & \frac{1}{M_{2}} & 0 \\ 0 & \frac{D_{7}}{M_{3}} & \frac{(-D_{7}+D_{9})}{M_{3}} & 0 & \frac{-1}{M_{3}} & \frac{1}{M_{3}} \\ -K_{4} & K_{4} & 0 & 0 & 0 & 0 \\ f_{6}(\tau) \\ f_{6}(\tau) \end{bmatrix} = \begin{bmatrix} \delta_{1}(\tau) \\ \delta_{2}(\tau) \\ \delta_{3}(\tau) \\ \delta_{3}(\tau) \\ f_{4}(\tau) \\ 0 \\ 0 \\ 0 \\ K_{6}(\tau) \end{bmatrix}$$

5.0 AN APPLICATION OF THE GIMBAL SYSTEM STATE MODEL

In the previous section, the state model for a gimbal system was developed. This section presents the use of the state model in formulating the design criteria utilized in the vibration analysis of gyros and accelerometers. In pursuing this end, a typical IMU will be considered.

5.1 TERMINAL EQUATION PARAMETERS

The IMU to be considered herein is shown in Figure 9. It is an inside-out platform with a dumbbell configuration. The mechanical system and system graph can be represented as shown in Figure 8. Hence, it remains to establish the parameters in the terminal equations.

The IMU considered is a combination of aluminum and stainless steel with the bulk of the structure being aluminum. The weight of the individual gimbals, including all components on that gimbal, are as follows:

Inner gimbal	13.80	lbs.
Middle gimbal	3.42	lbs.
Outer gimbal	6.99	lbs.
Case	27.39	lbs.

In determining the spring constants, the contribution from both the gimbal structure and the bearings utilized in the gimbals are considered. Therefore, the total spring constant is made up of the individual elements in series. Thus, the terminal equation involving the spring constants is as follows:

$$\frac{\mathrm{d}}{\mathrm{d}t} \begin{bmatrix} \mathbf{f}_{4}(t) \\ \mathbf{f}_{6}(t) \\ \mathbf{f}_{8}(t) \end{bmatrix} = \begin{bmatrix} K_{4} & 0 & 0 \\ 0 & K_{6} & 0 \\ 0 & 0 & K_{8} \end{bmatrix} \begin{bmatrix} \dot{\delta}_{4}(t) \\ \dot{\delta}_{6}(t) \\ \dot{\delta}_{8}(t) \end{bmatrix}$$

where

$$\frac{1}{K_i} = \frac{1}{K_G} + \frac{1}{K_B}$$

and

 K_{i} = the ith spring constant

K_G = the spring constant of the ith
 gimbal structure

K_B = the spring constant of the ith
 bearing

All of the platform gimbals are considered to be constructed of aluminum with the exception of the inner gimbal which is stainless steel. The specification for both kinds of material is as follows:

Aluminum

Density	0.097	lbs/in ³

Stainless Steel

		•
Density	Λ 2Λ	lbs/in ³
Densirv	11 /4	ing/in-

The spring constants for each gimbal were calculated. For the inner gimbal the structure was assumed to be a cantilever beam. For the middle and outer gimbals a simple beam supported at both ends with a concentrated load at the center was assumed. The resulting spring constants were found to be:

Inner Gimbal	$5.5 \times 10^{5} \text{ lbs/in}$

Middle Gimbal
$$1.4 \times 10^4$$
 lbs/in

Outer Gimbal 2.1×10^4 lbs/in

The bearings used in the gimbal system for this application are roller bearing type having a contact angle of 25° (contact angle is the angle made by a line passing through points of contact of the ball and both raceways with a plane perpendicular to the axis of the bearing when both races are centered with respect to each other). The spring constant for the bearings is dependent upon the direction of loading, i.e. axial or radial loading. Graphs of the bearing deflection versus load for both axial loads and radial loads with a contact angle of 25° are shown in Figures 10 and 11. For the specific condition used in this case, the spring constants were found to be

Axial Load 5×10^5 lbs/in

Radial Load 8.3×10^5 lbs/in

As can be seen from the graphs, the relationship between the deflection and load is nonlinear, but since the operation is over a small range, the relationship may be considered linear. If a different operating point is selected, the bearing spring constant may be changed. This change is operating point is accomplished through the use of bearing pre-load (bearing pre-load is a means by which the bearing can be placed under an initial load).

After the appropriate combination of the material spring constant and bearing spring constant was made according to the

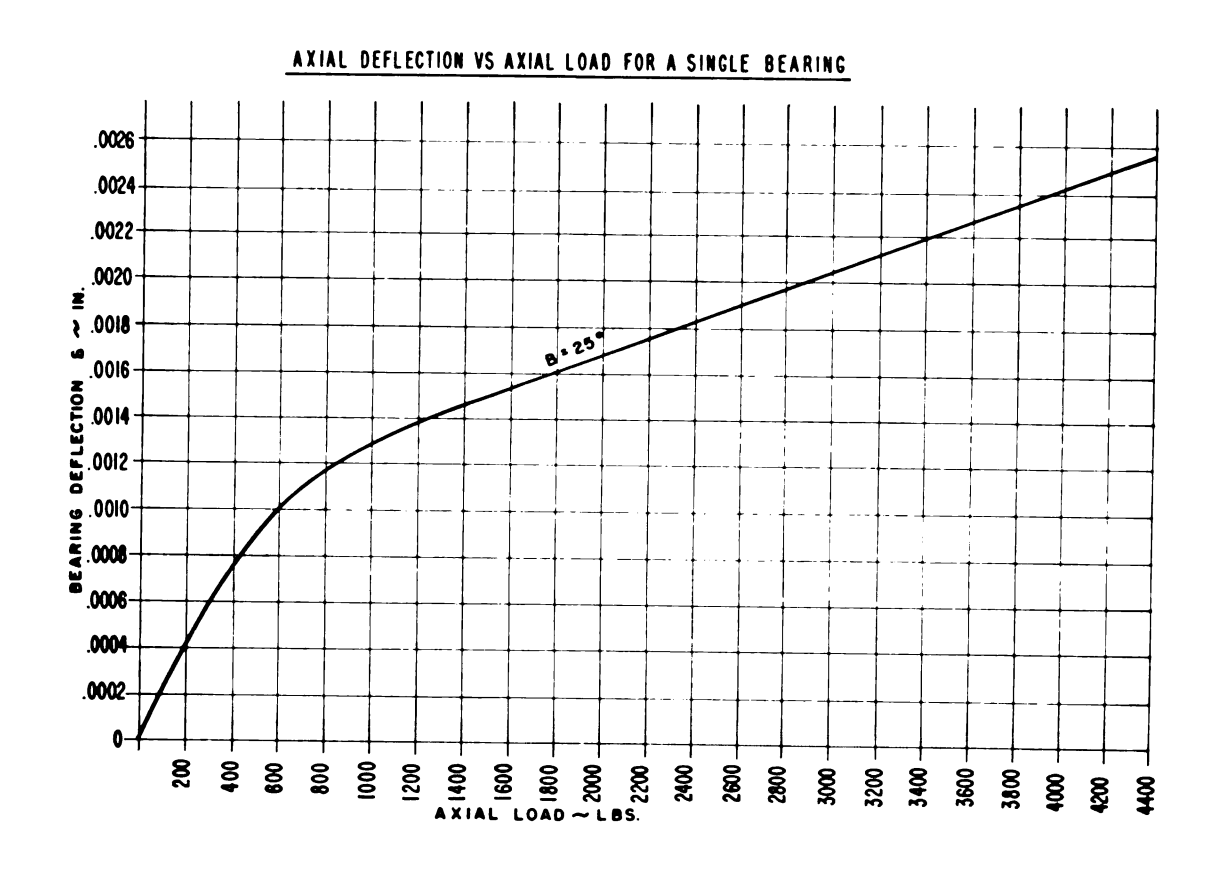


FIGURE 10

AXIAL DEFLECTION VS. AXIAL LOAD FOR A SINGLE BEARING

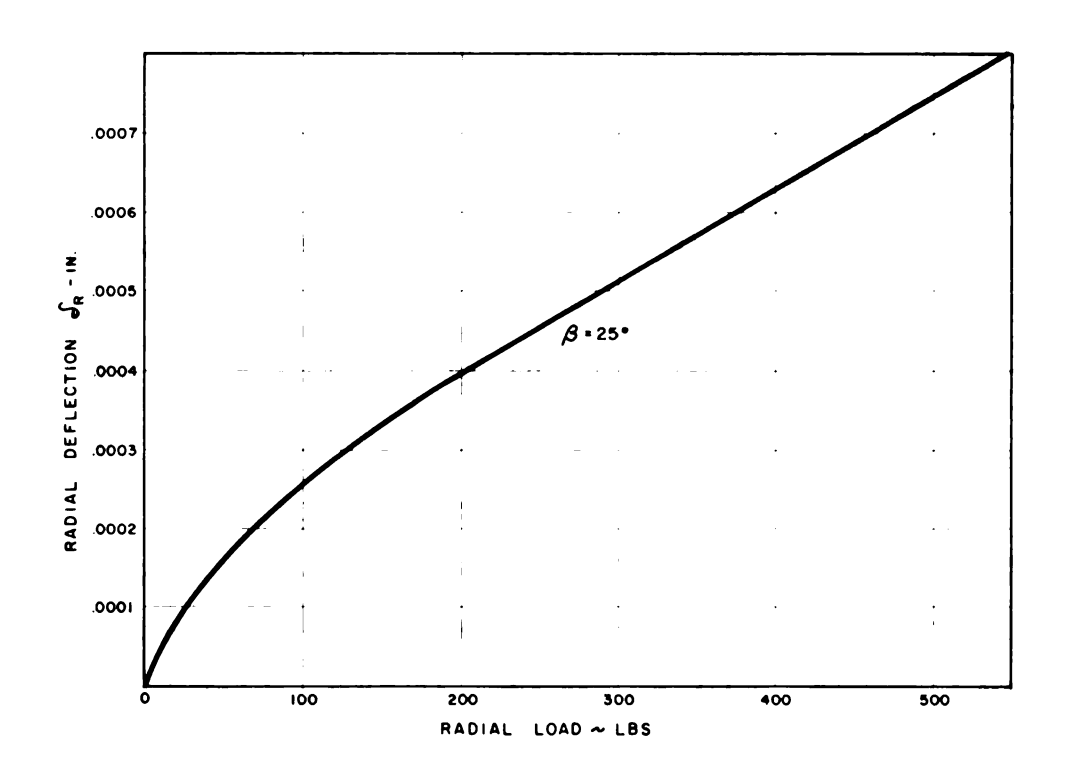


FIGURE 11

RADIAL DEFLECTION VS. RADIAL LOAD FOR A SINGLE BEARING

system model, the gimbal spring constants to be used in the terminal equations were found to be:

Inner Gimbal 10.3×10^4 lbs/in

Middle Gimbal 1.39×10^4 lbs/in

Outer Gimbal 4×10^4 lbs/in

The last parameter to be considered is the damping coefficient. It has been found through experience with other gimbal systems that this parameter is small in comparison to the spring constant and the mass of the gimbals. The system damping is provided by the combination of structural damping and windage effects which are minimal factors. Experience has shown that the damping ratio may range from .01 to .06 for a platform gimbal system.

5.2 SOLUTION OF THE STATE MODEL

The primary objective of this analysis is to determine the system resonant frequencies and, consequently, a simplified procedure may be used to solve the state model. This method consists in triangularizing the coefficient matrix to obtain an explicit expression for a sub-set of the variables in the state vector. The sub-set provides the desired information.

Consider the state model which can be represented as follows:

$$\frac{d}{dt} X(t) = A X(t) + E(t)$$

Taking the Laplace transform gives:

$$s X(s) = A X(s) + X(o) + E(s)$$

or

$$[s U - A] X(s) = X(o) + E(s)$$

then

$$X(s) = [s U - A]^{-1} (X(o) + E(s))$$

In this example all initial conditions are considered as zero. The coefficient matrix after application of the Laplace transform is

$$\begin{bmatrix} s + \frac{D_5}{M_1} & \frac{D_5}{M_1} & 0 & \frac{1}{M_1} & 0 & 0 \\ \frac{D_5}{M_1} & s + \frac{D_5 + D_7}{M_2} & \frac{D_7}{M_2} & \frac{-1}{M_2} & \frac{1}{M_2} & 0 \\ 0 & \frac{D_7}{M_3} & s + \frac{D_7 + D_9}{M_3} & 0 & \frac{-1}{M_3} & \frac{1}{M_3} \\ -\kappa_{l_1} & \kappa_{l_1} & 0 & s & 0 & 0 \\ 0 & -\kappa_6 & \kappa_6 & 0 & s & 0 \\ 0 & 0 & -\kappa_8 & 0 & 0 & s \end{bmatrix} \begin{bmatrix} \delta_1(s) \\ \delta_2(s) \\ \delta_3(s) \\ \delta_3(s) \\ -\epsilon_{l_1} & \epsilon_{l_2} & \epsilon_{l_3} & \epsilon_{l_4} \\ -\epsilon_{l_5} & \epsilon_{l_5} & \epsilon_{l_5} & \epsilon_{l_5} \\ -\epsilon_{l_5} & \epsilon_{l_5} & \epsilon_{l_5} \\ -\epsilon_{l_5}$$

After manipulation on the rows the result is:

$$\begin{bmatrix} \frac{M_{1}s^{2}+D_{5}s-K_{i_{4}}}{M_{1}s} & \frac{D_{5}s-K_{i_{4}}}{M_{1}s} & 0 & 0 & 0 & 0 \\ \frac{D_{5}s-K_{i_{4}}}{M_{2}s} & \frac{M_{2}s^{2}+(D_{5}+D_{7})s+(K_{i_{4}}+K_{6})}{M_{2}s} & \frac{D_{7}s-K_{6}}{M_{2}s} & 0 & 0 & 0 \\ 0 & \frac{D_{7}s-K_{6}}{M_{3}s} & \frac{M_{3}s^{2}+(D_{7}+D_{9})s+(K_{6}+K_{8})}{M_{3}s} & 0 & 0 & 0 \\ -K_{i_{4}} & K_{i_{4}} & 0 & s & 0 & 0 \\ 0 & -K_{6} & K_{6} & 0 & s & 0 \\ 0 & 0 & -K_{6} & 0 & s & 0 \\ \end{bmatrix} \begin{bmatrix} \delta_{1}(s) \\ \delta_{2}(s) \\ \delta_{3}(s) \\ f_{1}(s) \\ f_{2}(s) \end{bmatrix} = \begin{bmatrix} 0 \\ 0 \\ \frac{\delta_{3}(s)}{M_{3}s} \\ 0 \\ 0 \\ 0 \\ 0 \\ K_{6} \end{bmatrix}$$

The first three equations are independent of the last three and consequently the resonant frequencies may be solved much more simply. Considering only the first three rows and multiplying each by M_1 s, M_2 s, and M_3 s, respectively, results in the set:

$$\begin{bmatrix} M_{1}s^{2} + D_{5}s + K_{i_{4}} & D_{5}s - K_{i_{4}} & 0 \\ D_{5}s - K_{i_{4}} & M_{2}s^{2} + (D_{5} + D_{7})s + K_{i_{4}} + K_{6} & D_{7}s - K_{6} \\ 0 & D_{7}s - K_{6} & M_{3}s^{2} + (D_{7} + D_{9})s + (K_{6} + K_{8}) \end{bmatrix} \begin{bmatrix} \dot{\delta}_{1}(s) \\ \dot{\delta}_{2}(s) \\ \dot{\delta}(s) \end{bmatrix} = \begin{bmatrix} 0 \\ 0 \\ D_{9}s - K_{8} \end{bmatrix}$$

The characteristic equation may be solved for the resonant frequencies by a number of methods. Substitution of the parameters established previously into the above equations will provide the system characteristics.

To facilitate limit checks and hand calculations it should be noted that ζ <<1 and, therefore, can be assumed to be zero. This leads to little error in computing the resonant frequencies since:

$$\omega_{\rm D} = \omega_{\rm n} \sqrt{1-\zeta^2}$$

To determine the transmissibility (this is the ratio of the amplitude of displacement transmitted to the impressed displacement) at the resonant frequencies, the following approximation* can be used:

Transmissibility
$$\cong \frac{1}{2\zeta}$$

A reasonable estimate for the damping ratio (ζ) applicable to the case under consideration is 0.05. Consequently the transmissibility at the resonant frequencies is assumed to have a nominal value of 10.

^{*} This is exact for a second-order system.

The sub-set may now be easily solved by taking the inverse matrix as follows:

$$\begin{bmatrix} \dot{\delta}_{1}(s) \\ \dot{\delta}_{2}(s) \\ \dot{\delta}_{3}(s) \end{bmatrix} = \frac{1}{D(s)} \quad A(s) \begin{bmatrix} 0 \\ 0 \\ D_{9}s - K_{8} \end{bmatrix}$$

where D(s) is the characteristic polynominal and A(s) is the adjoint matrix. From this expression the transfer function of the inner gimbal response to an excitation on the case may be obtained. If the damping coefficients are considered zero, the transfer function is found to be:

$$\frac{\delta_{1}(s)}{\delta_{10}(s)} = \frac{K_{4}K_{6}K_{8}}{\begin{bmatrix} M_{1}s^{2}+D_{5}s+K_{4} & D_{5}s-K_{4} & 0 \\ D_{5}s-K_{4} & M_{2}s^{2}+(D_{5}+D_{7})s+K_{4}+K_{6} & D_{7}s-K_{6} \\ 0 & D_{7}s-K_{6} & M_{3}s^{2}+(D_{7}+D_{9})s+K_{6}+K_{8} \end{bmatrix}}$$

Solving the characteristic equation (assuming zero damping coefficients) with the parameters previously established results in the following resonant frequencies:

$$\omega_1$$
 = 850 rad/sec f_1 = 135 cps

$$\omega_2 = 1730 \text{ rad/sec}$$
 $f_2 = 275 \text{ cps}$

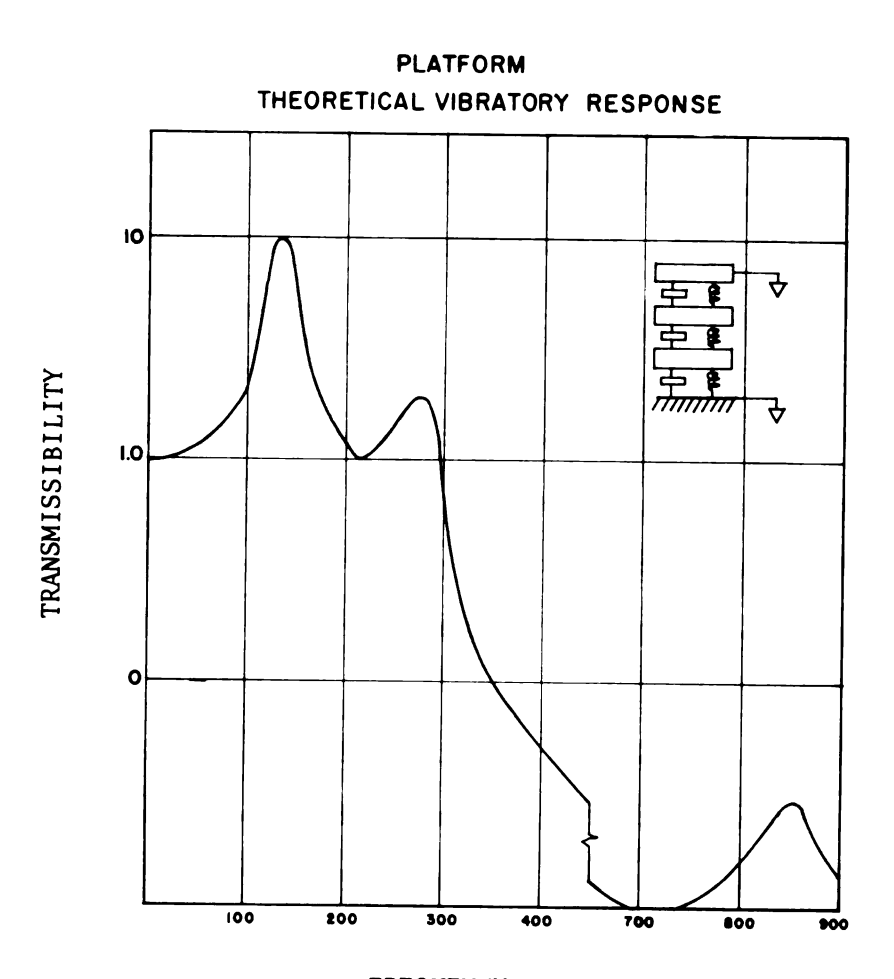
$$\omega_3$$
 = 5330 rad/sec f_3 = 850 cps

A plot of the transmissibility for the gimbal system is shown in Figure 12 where the resonant frequencies are those given above and the amplitude of the transmissibility at each frequency was computed using the approximation of $\zeta = .05$.

5.3 DESIGN CONSIDERATIONS

The obvious objective in the design of a stable platform from the environmental standpoint is to provide as low a response to vibration as possible. This condition necessitates the minimization of the transmissibility, and requires attenuation over a large portion of the frequency spectrum. Commensurate with this objective, several basic factors should be considered:

1. Damping coefficient - This is mainly a function of the material used in the design. A damping ratio range of 0.02 to 0.05 means a transmissibility range of 25 to 10. Hence, this factor should be a critical item when considering the material to be used.



FREQUENCY - CPS

FIGURE 12

PLATFORM
THEORETICAL VIBRATORY RESPONSE

- 2. Gimbal frequencies No two gimbals should have the same resonant frequencies. The octave rule should apply whereby the frequencies are to be kept an octave apart. In this way, the possibility of two resonant frequencies lying on top of each other is avoided.
- 3. Instrument natural frequencies The natural frequencies of the instrument mounted on the platform should not coincide with the gimbal natural frequency, and should be in a region where the attenuation provided by the platform furnishes adequate protection for the instrument.
- 4. Minimum resonant frequency Inasmuch as the platform will have a resonant rise at some point, the specific frequency must be considered in the design of stabilization loops and similar equipment which must function properly throughout the range of vibration.
- 5. Platform isolator An obvious method reducing vibration effects is the use of a platform isolator. However, this is by no means a simple solution since this adds an additional degree of freedom to the platform which may cause problems in the stabilization loops. In addition, adequate isolators are difficult to obtain without considerable time and expense, and provide another item that can fail.

6.0 EFFECT OF SINUSOIDAL VIBRATION ON PLATFORM INSTRUMENTS

To this point the main consideration has been the gimbal system. This was necessary since its characteristics shape the environment seen by the platform instruments which are located on the innermost gimbal known as the stable element. Now, considering the vibration on the stable element, the effects on the platform instruments will be considered. This section presents a description of the errors resulting from sinusoidal vibration in both accelerometers and gyros.

6.1 ACCELEROMETERS

The most common type of accelerometer used in inertial guidance is a pendulous force-balance type (Figure 13), and is the type considered here. This accelerometer consists of a pendulous mass which acts as the sensing element within a servo loop. Under gravitational attraction only, the mass hangs along the line of local gravity. Assume an acceleration (a) is now applied along a line perpendicular to the local gravity line. This produces a torque on the pendulum since

T = Pa

where P is the pendulosity. In this accelerometer a pickoff senses the motion of the pendulum, amplifies the signal, and then applies

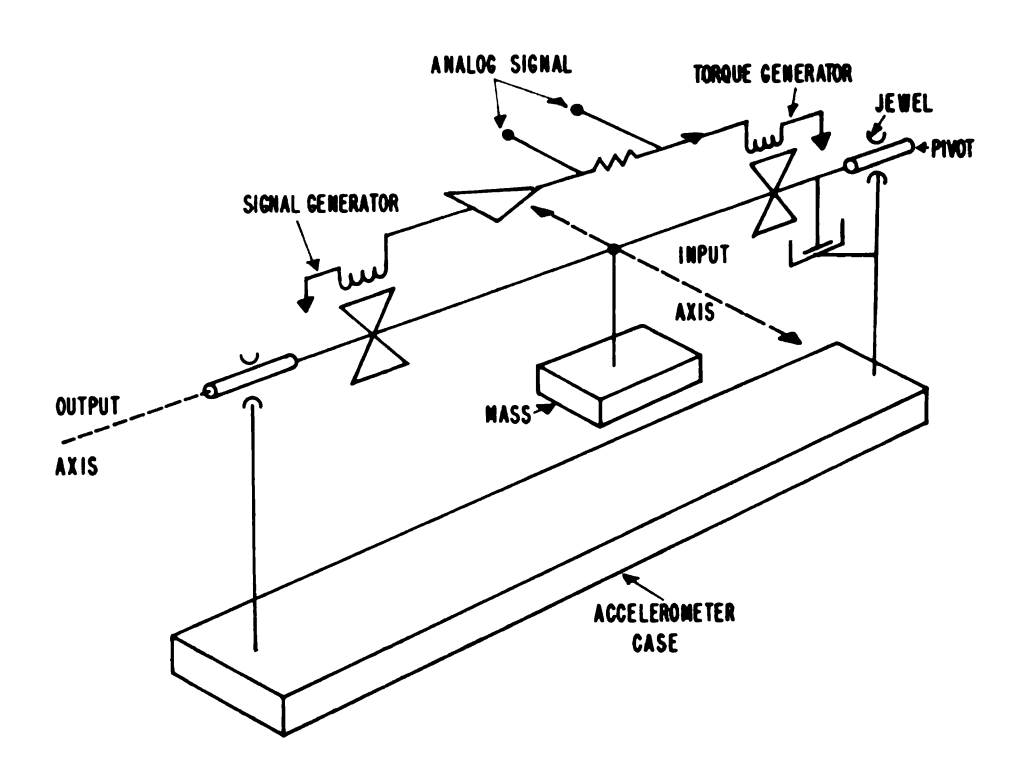


FIGURE 13

PENDULOUS FORCE - BALANCE ACCELEROMETER WITH ANALOG OUTPUT

it to a torquer which acts to counteract the torque. The torque produced by the torquer can be found from

$$T = K_T i$$

where $K_{\overline{T}}$ is torquer gain

and i is the current through the torquer

Therefore, a measure of the acceleration can be made by determining the current in the feedback loop since

$$i = \frac{P_a}{K_T} = Ka$$

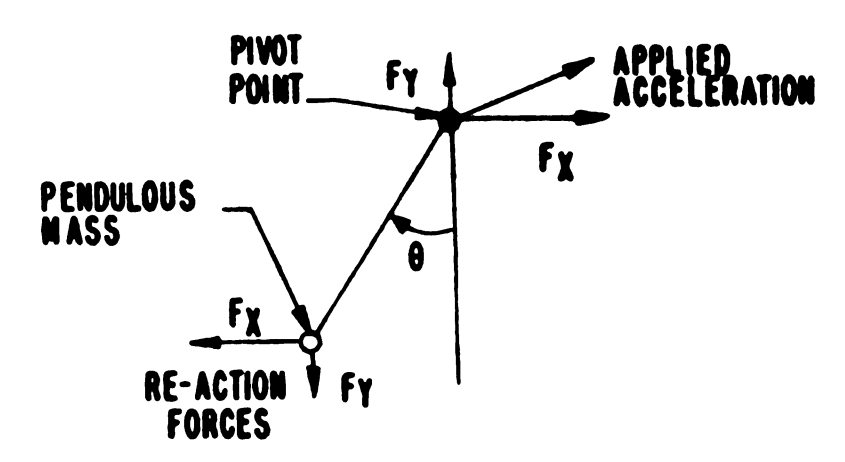
where

K represents the ratio
$$\frac{P}{K_T}$$

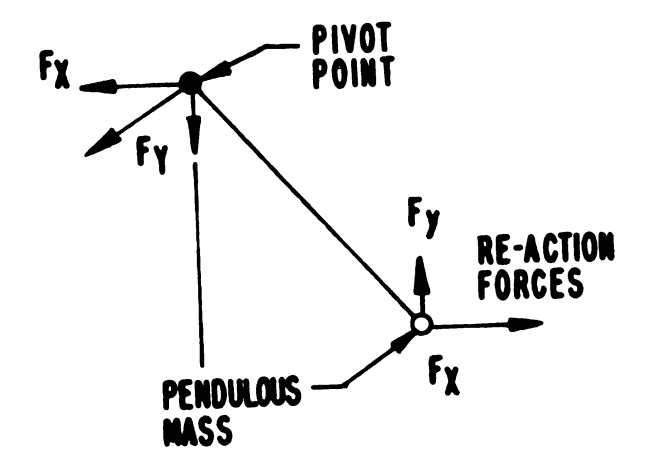
In an accelerometer there are three major sources of error. These are known as vibropendulous effects, nonlinearities, and scale factor variation. The first condition is inherent in the pendulous characteristic of the accelerometer. The other two are common to all types of accelerometers. Each of these errors will now be discussed.

6.1.1 <u>Vibropendulous Error</u>

The error produced by the pendulous characteristic of the accelerometer when subjected to a sinusoidal vibration can be readily seen by referring to the forces acting on a pendulum under an acceleration. If an acceleration upward and to the right is assumed, then the forces on the pendulum are as shown in the illustration and the resulting torque can be noted.



Now, if the acceleration is reversed (downward and to the left) it can be seen in both cases the torques due to the force along the X axis are in the opposite direction and therefore if the average torque is considered, these two torques would cancel.



However, the torques caused by the forces along the Y axis are in the same direction (counterclockwise) in either case and consequently are additive. This is known as vibropendulous torque which results in an accelerometer error.

For the pendulous force-balance accelerometer with analog output the vibropendulous torque can be described by the following expression:⁶

$$M = \frac{P^2 A^2 \delta \sin 2 \phi \cos \psi}{2}$$

where

M = vibropendulous torque dyne-cm

P = pendulosity

A = rms vibration

 δ = pendulum deflection rad/dyne-cm

 ϕ = line of applied vibration with respect to sensitive axis

 ψ = phase lag of the pendulum deflection relative to applied vibration

Several things can be noted immediately from the expression.

It is important to minimize the accelerometer pendulosity since the torque is proportional to the square of the pendulosity. The torque is also proportional to the square of the applied rms vibration. A high stiffness coefficient will reduce the effect on vibropendulosity.

The maximum error is at the 45° points. However, if the vibration is first along a 45° line and then along a 135° line, the resulting torques differ in direction and thereby cancel each other. The final item is, of course, the phase lag which should be considered as a possibility in reducing this error.

The above is a typical pendulous force-balance type of accelerometer. Another interesting type which is now becoming quite common is a pulse-rebalance accelerometer (Figure 14) which is quite similar to the one already described. The difference lies in the operation of the accelerometer which provides the restoring torque in the form of pulses rather than as a continuous analog signal. Consequently, whenever some minimum threshold level is exceeded by the motion of the pendulum, a fixed pulse of energy is applied to the torquer thereby forcing the pendulum back to the nominal position. Depending on the particular parameters, then, each pulse is equivalent to an increment of velocity. By summing these pulses, the total velocity at any time can be determined.

Vibropendulous torque also exists in this type of accelerometer but the effects are not as great. This can be seen by considering such an accelerometer being subjected to a sinusoidal vibration along a line at some angle ϕ to the sensitive axis.

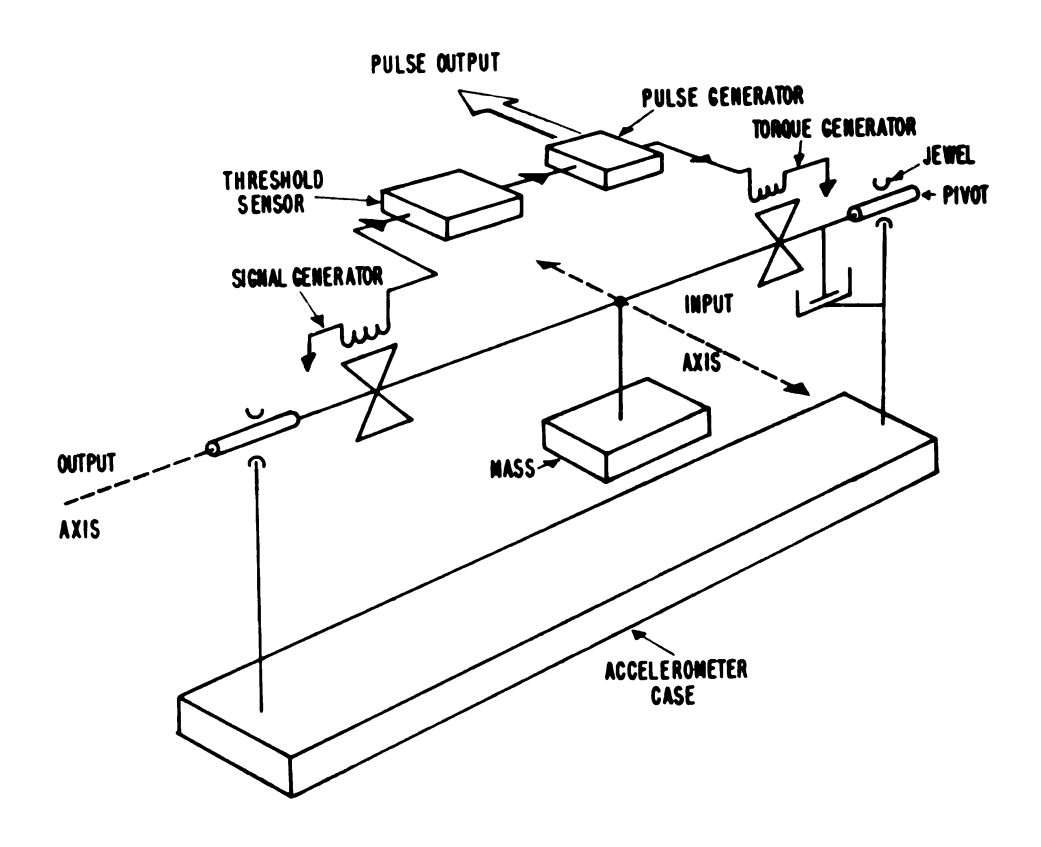
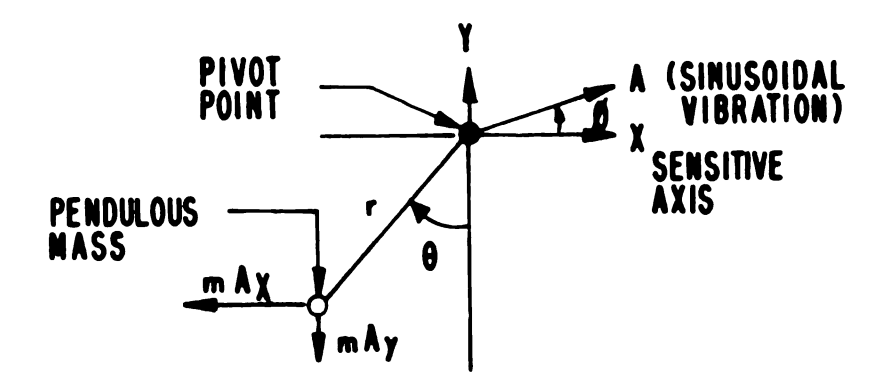


FIGURE 14

PENDULOUS FORCE - BALANCE ACCELEROMETER WITH PULSE OUTPUT



Since the force along the Y axis was shown to produce the vibropendulous torque, this can be found to be

$$M = m A_y r \sin \theta$$

The motion of the pendulum is small; therefore, it is appropriate to let $\sin \theta = \theta$. In addition, the pendulosity, mr, is a constant of the accelerometer which allows the above expression to be re-written as

$$M = P A_y \theta$$

Thus it can be seen that the vibropendulous torque is a function of the pendulosity, the applied vibration and the pendulum swing. In the case under consideration the applied vibration is a sinusoidal vibration; therefore, let

$$A_y(t) = A_y \sin \omega t$$

Since the pendulum swing associated with a sinusoidal vibration is also sinusoidal and, taking into account the phase lag, the pendulum swing can be written as

$$\theta(t) = \theta \sin(\omega t - \psi)$$

where

$$\psi$$
 = phase lag

Substituting the expressions for the applied vibration and pendulum swing into the above equation for vibropendulous torque results in

$$M(t) = P A_{y} \sin \omega t \left[\theta \sin (\omega t - \psi) \right]$$

By trigonometric identities this reduces to

$$M(t) = \frac{P A \theta}{2} \left[\cos \psi - \cos (2\omega t - \psi) \right]$$

Since the average torque is desired and the average contribution to the torque by the cyclical term is zero, the average torque can be written as

$$M_{avg} = \frac{P A_y \theta \cos \psi}{2}$$

Since $A_y = A \sin \phi$, where A is the amplitude of the total vibration input, the above becomes

$$M_{avg} = \frac{P A \theta \sin \phi \cos \psi}{2}$$

where

M = vibropendulous torque, dyne-cm

P = pendulosity, gm-cm

 θ = threshold level, radians

A = amplitude of vibration, cm/sec^2

 ϕ = angle of applied vibration with sensitive axis

 ψ = phase lag of the pendulum

The pulse torquing approach appears to have reduced the susceptibility to vibration effects. In this case, the vibropendulous torque can be seen to be proportional to the pendulosity and the applied vibration whereas previously, it was shown to be dependent upon the square of each of these factors (in most cases operation of the accelerometer requires that P > 1). The torque is also a function of the pendulum swing which for this type of accelerometer is a constant. Reduction in the threshold level (pendulum swing) produces a proportional decrease in the vibropendulous torque. The final difference to be noted is the dependency of the torque on ϕ rather than 2 ϕ . Therefore, the maximum torque will be produced by an applied vibration lying essentially along a line perpendicular

 $(\phi < 90^{\circ})$ to the sensitive axis of the accelerometer. The requirement for ϕ to be less than 90° stems from the need for a small component of acceleration along the X axis which is necessary to drive the pendulum off of the null position.

6.1.2 Nonlinearities

Another characteristic of the accelerometer that is important when considering vibration is the nonlinearity in gain that may exist. It will be shown that an error is produced by the nonlinear terms due to rectification effects.

Consider the output of an accelerometer to be described by the following expression:

$$V = K_0 + K_1 A + K_2 A^2 + K_3 A^3 + \cdots$$

where

V = accelerometer output in volts

A = acceleration input

 K_0 = bias terms

 K_1 = scale factor

 K_2 = coefficient of second order nonlinearity

 K_3 = coefficient of third order nonlinearity

Assume the acceleration input consists of thrust acceleration and vibration. This can be represented by

$$A = A_T + A_V \sin \omega t$$

Substitution into the above expression with consideration given only to the second order nonlinearity (assuming the higher terms are negligible) and terms including vibrations yields

$$V = 2K_2 A_T A_V \sin \omega t + K_2 A_V^2 \sin^2 \omega t$$

or

$$V = 2K_2 A_T A_V \sin \omega t + \frac{K_2 A_V^2}{2} (1-\cos 2 \omega t)$$

Taking the average and considering only complete cycles results in the error produced by vibration as

$$V = \frac{K_2 A_V^2}{2}$$

However, an important aspect of the two terms dropped should not be overlooked. Although the average value of each term can be seen to be essentially zero, the amplitude of the error contribution can be significant. Therefore this could lead to saturation of the accelerometer and additional errors. For purposes of this thesis, it is assumed that the accelerometer is not saturated and that the above error equation holds.

6.1.3 Scale Factor Error

The particular characteristic of an accelerometer defined as scale factor was noted previously. Here it will be shown how such a characteristic of a pulse-rebalance accelerometer generates an error under sinusoidal vibration.

Consider the expression for the pulse-rebalance accelerometer as follows:

$$P = K At$$

where

P = accelerometer output in pulses

K = scale factor pulses/sec/g

A = acceleration input

g = gravity

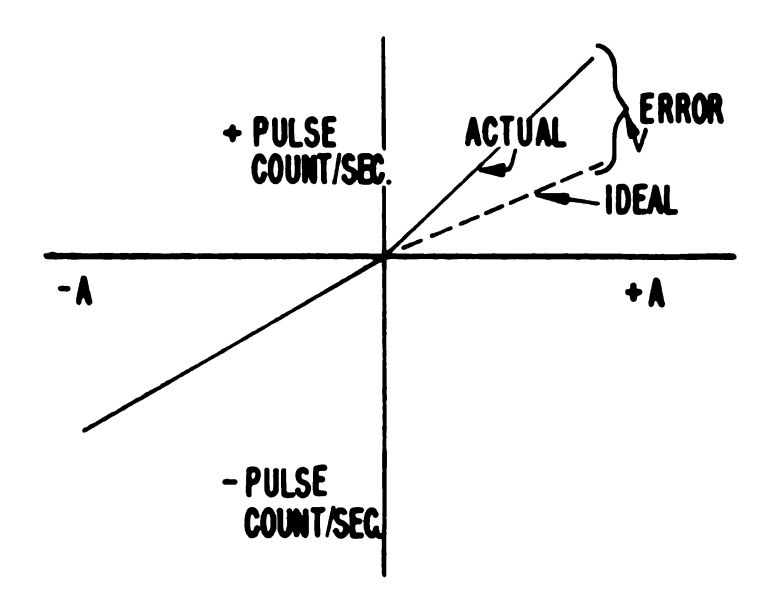
t = time in sec.

Since the accelerometer is designed such that each pulse is equivalent to a specific value of velocity, the total velocity can be found by performing an algebraic summation, or

$$V = \sum_{i=1}^{N} P_{i}$$

where N = total number of increments of velocity

The point under consideration here is that the scale factor is different for the positive and negative sides of the accelerometer as shown in the figure. Consequently under a sinusoidal vibration the difference between the two slopes will result in an error.



This can be seen by considering the above expression with two different slopes as

$$P = K_1 A_1 t_1 - K_2 A_2 t_2$$

where the subscripts refer to the polarity. Assuming a sinusoidal vibration, the following holds:

$$A_1 = A_2 = A$$

$$t_1 = t_2 = t$$

then

$$P = (K_1 - K_2) At$$

The velocity error produced by this is

$$V = \sum_{i=1}^{N} (K_1 - K_2) At_i$$

Therefore, in spite of the fact that the input vibration has a zero mean, an extensive error can be built up due to vibration.

This aspect is particularly important in inertial guidance systems since a common guidance technique utilized is to fly a trajectory such that the cross-axis acceleration is held to zero.

Under this condition the cross-track accelerometer will be subjected to vibration inputs and could produce significant errors.

The discussion of the effects of sinusoidal vibration on accelerometers is now complete. The next section will present the specific considerations of gyros under vibration.

6.2 GYROS

The drift in gyro performance is categorized into two major groups⁹: non-g-sensitive drift, and g-sensitive drift. The first category is unaffected by vibration, and consequently this section will be concerned only with g-sensitive drift as produced by sinusoidal vibration.

The g-sensitive drift is further divided into two groups:

1) drift due to mass unbalance, and 2) drift due to anisoelastic effects. Each of these will be considered in relation to vibration.

6.2.1 Mass Unbalance Drift

One effect of sinusoidal vibration on gyros can be seen by considering the expression for gyro drift due to mass unbalance:

$$\dot{\phi} = \frac{K_1}{T} \int_{0}^{T} Adt$$

where

 ϕ = drift rate in deg/hr

K₁ = error coefficient due to mass
unbalance deg/hr/g

A = total acceleration, g's

If the total acceleration is again considered to be composed of the thrust acceleration and a sinusoidal vibration then:

$$\dot{\phi} = \frac{K_1}{T} \int_{0}^{T} (A_T + A_V \sin \omega t) dt$$

or

$$\dot{\phi} = \frac{K_1}{T} \left[\left(A_T t - \frac{A_V}{\omega} \cos \omega t \right) \right]_0^T$$

The first term is the error produced by the thrust acceleration and is normally considered in error analyses. The second term can be seen to have a zero average contribution. Hence, it can be concluded that sinusoidal vibration will produce no steady-state error from the mass unbalance coefficient.

It is interesting to consider if this conclusion is upheld by applying an equation for a pendulous mass of an accelerometer. That is, the mass unbalance of the gyro can be viewed as a pendulous mass about the output axis; therefore, it is reasonable to ask if a vibropendulous error is also incurred. This may be answered by considering the expression for vibropendulous torque of a pendulous force-balance accelerometer as presented in Section 6.1.1:

$$M = \frac{P^2 A^2 \delta \sin 2 \phi \cos \psi}{2}$$

where

M = vibropendulous torque dyne-cm

P = pendulosity

A = rms vibration

 δ = pendulum deflection rad/dyne-cm

 ϕ = line of applied vibration with respect to the sensitive axis

 ψ = phase lag of the pendulum deflection to the applied vibration

The particular parameter that must be determined is the pendulum deflection. The relationship between torque and the gyro output axis angle can be seen from the transfer function

$$\frac{\rho}{T} = \frac{1/D}{s(\tau s + 1)}$$

where

 τ = time constant, I/D

ρ = gyro angular displacement

T = torque input

For most gyros the time constant is approximately equal to one, and in addition, the damping coefficient is much greater than one. Therefore, from these considerations it can be seen that any sinusoidal input signals would be greatly attenuated. Hence, under these conditions, the vibropendulous torque due to mass unbalance is insignificant and corroborates the previous analysis.

6.2.2 Anisoelastic Drift

The anisoelastic drift due to sinusoidal vibration can be seen by considering the following equation:

$$\dot{\phi} = \frac{K_2 \sin 2 \theta}{T} \int_0^T A^2 dt$$

where

 ϕ = drift rate in deg/hr

K₂ = error coefficient due to anisoelastic
 effect in deg/hr/g²

θ = angle the input axis makes with the applied vibration

A = total acceleration, g's

For the case where the total acceleration acting on the gyro is composed of the thrust acceleration and sinusoidal vibration, the drift error is found to be

$$\dot{\phi} = \frac{K_2 \sin 2\theta}{T} \int_0^T \left[A_T^2 + 2A_T A_V \sin \omega t + A_V^2 \sin^2 \omega t \right] dt$$

The first term is the error contributed by the thrust acceleration and shall not be considered further. The second term can be seen to result in an average contribution of zero. The third term results in the following

$$\dot{\phi} = \frac{K_2 A_V^2 \sin 2\theta}{T} \left[-\frac{1}{2\omega} \cos \omega t \sin \omega t + \frac{1}{2} t \right]_0^T$$

or

$$\dot{\phi} = \frac{K_2 A_V^2 \sin 2\theta}{2}$$

It should be noted that - due to the sine term - the drift rate of the gyro is sensitive to the direction of applied vibration. In some cases, where the direction is changing, some cancellation can occur.

This completes the analysis of the major platform instruments in relation to sinusoidal vibration. The system error due to the combination of each of the platform instrument errors is treated in the next section.

7.0 SYSTEM ERROR DUE TO SINUSOIDAL VIBRATION

The ultimate objective of the analyses carried out herein is the formulation of the equation for the total system error due to a sinusoidal vibration present on the case of the IMU. This section presents the development of such an equation.

From the standpoint of vibration effects the IMU has been considered to consist of three major components:

- 1. a gimbal structure
- 2. accelerometers
- 3. gyros

Each of these has been treated in the preceding sections but it remains to establish their relationships to the system error. Refer to Figure 15. The system error is seen to be the error existing in the accelerometer output, and is dependent upon the three major components. With a given vibration on the case of the IMU the gimbal structure serves to shape the vibration seen by both the gyros and the accelerometers. Consequently the susceptibility to vibration of the gyros and accelerometers, in turn, produce errors in performance.

The accelerometer error adds directly to the system error whereas the gyro errors have an indirect effect. The errors in the gyros cause the stable platform to lose its orientation (tilt) thereby introducing coupling errors in the accelerometers. The errors

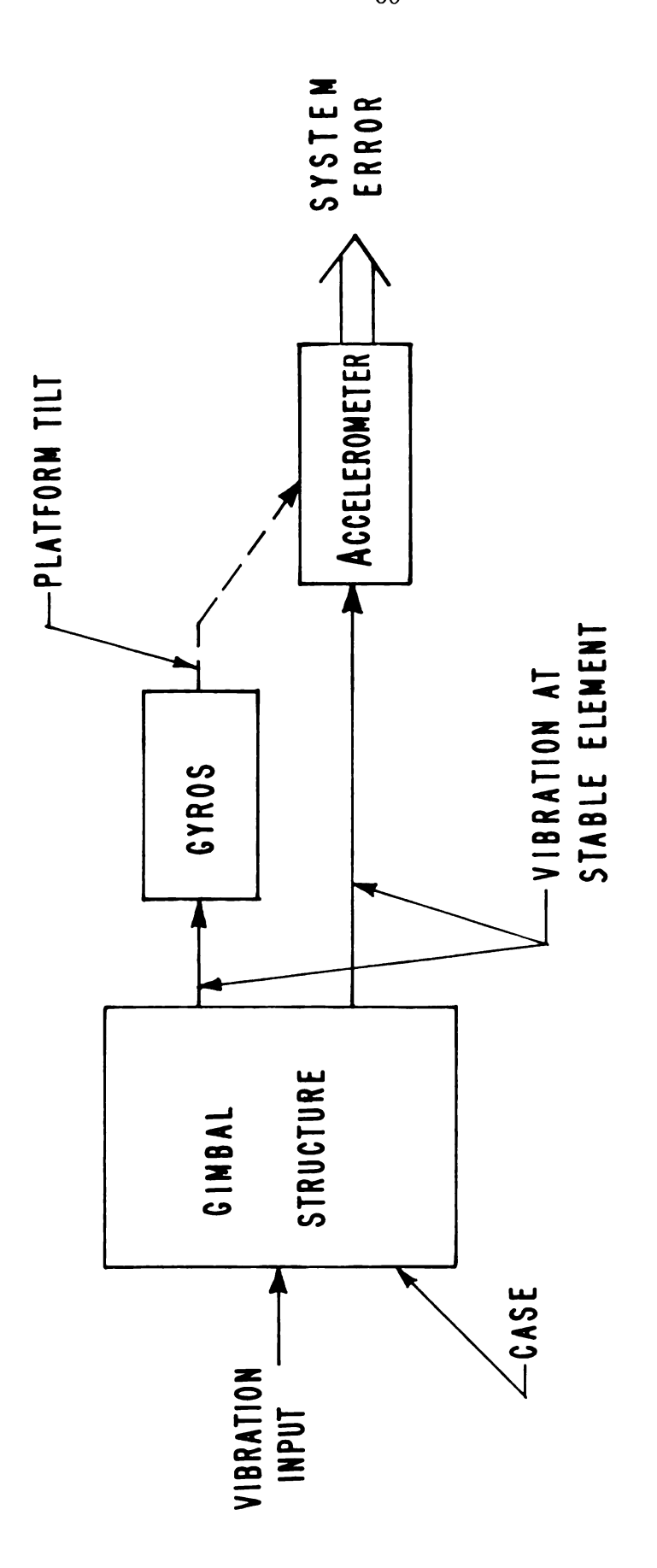


FIGURE 15

SYSTEM ERROR MODEL

consist of either gravity coupling or thrust coupling which produce additional errors in the accelerometer output. The system error equation reflecting these effects will be shown.

The vibration on the case of the IMU is modified by the gimbal structure was developed in Section 4.0 with an example given in Section 5.0; it will not, therefore, be repeated here. The technique as illustrated in those sections serves to determine the vibration on the accelerometers and gyros.

The accelerometer was shown to have three types of errors:

1) vibropendulous error, 2) non-linearity, and 3) scale factor error. Since the errors in the accelerometers contribute directly to the system error, the error equations as derived in Section 6.1 can be considered directly. The error equations for a pendulous, pulse-rebalance accelerometer are as follows where the acceleration error is given by (refer to Sections 6.1.1 and 6.1.2)

$$\begin{bmatrix} A_{\mathbf{X}} \\ A_{\mathbf{y}} \end{bmatrix} = \begin{bmatrix} \frac{\theta \sin \phi \cos \psi}{2} & 0 & 0 \\ 0 & \frac{\theta \sin \phi \cos \psi}{2} & 0 \\ 0 & 0 & \frac{\theta \sin \phi \cos \psi}{2} \end{bmatrix} \begin{bmatrix} A_{\mathbf{X}} \\ A_{\mathbf{y}} \end{bmatrix} \cdot \begin{bmatrix} \frac{\kappa_{2x}}{2k_{1x}} & 0 & 0 \\ 0 & \frac{\kappa_{2y}}{2k_{1y}} & 0 \\ 0 & 0 & \frac{\kappa_{2z}}{2k_{1z}} \end{bmatrix} \begin{bmatrix} A_{\mathbf{X}}^2 \\ A_{\mathbf{y}}^2 \end{bmatrix}$$

and the velocity error is (refer to Section 6.1.3)

$$\begin{bmatrix} v_{x} \\ v_{y} \\ v_{z} \end{bmatrix} = \begin{bmatrix} \sum_{i=1}^{n} (K_{1} - K_{2}) t_{i} & 0 & 0 \\ 0 & \sum_{i=1}^{n} (K_{1} - K_{2}) t_{i} & 0 \\ 0 & 0 & \sum_{i=1}^{n} (K_{1} - K_{2}) t_{i} \end{bmatrix} \begin{bmatrix} A_{x} \\ A_{y} \\ A_{z} \end{bmatrix}$$

The drift error produced in the gyros was shown to be produced by the effect of vibration on the anisoelastic characteristics of the gyros (see Section 6.2) and was found to be

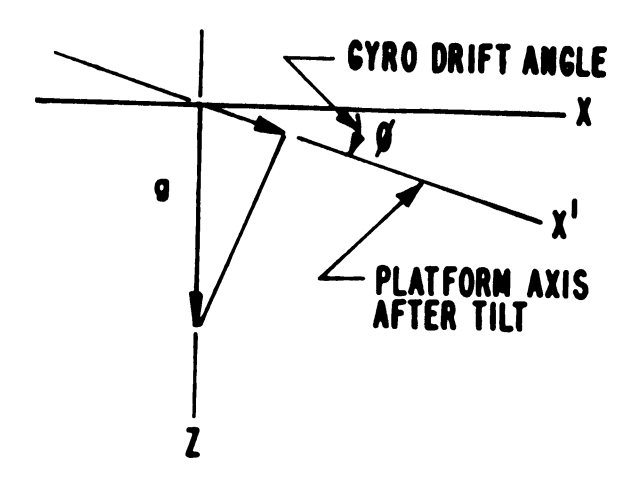
$$\dot{\phi} = \frac{K_2 A_V^2 \sin 2\theta}{2}$$

The gyro drift produces a tilt in the stable platform which causes a component of either gravity or the thrust vector to be sensed by the

accelerometer. This can be seen by referring to the figure. The component of gravity sensed by the accelerometer because of the gyro drift angle is

$$X = g \sin \phi$$

Since ϕ is small then this can be written as



The acceleration can be expressed as a function of the gyro drift rate error as

$$\ddot{X}(t) = \frac{g \dot{\phi} t}{57.3 \times 3600}$$

where t is the time duration in seconds over which the vibration acts on the gyro and the 57.3 and 3600 factors correspond respectively to conversions from degrees to radians and hours to seconds.

Replacing the gyro drift rate error by the expression given above yields

$$X(t) = \frac{g t K_2 A_V^2 \sin 2\theta}{2 \times 57.3 \times 3600}$$

One further item needs to be considered before the expression for the gyro errors can be written. This is the coupling produced by each gyro. From a consideration of the drift of each of the gyros it can be found that the X axis accelerometer will sense a component of gravity and the Z axis accelerometer will sense a component of the thrust vector. In the case of the Y accelerometer a component of both the thrust vector and the gravity vector is sensed. Then, the error equation can be written as

$$\begin{bmatrix} A_{x} \\ A_{y} \end{bmatrix} = \begin{bmatrix} 0 & \frac{g \text{ t K} \sin 2\theta}{412,560} & \frac{g \text{ t K} \sin 2\theta}{412,560} \\ \frac{T \text{ t K} \sin 2\theta}{412,560} & \frac{(g+T) \text{ t K} \sin 2\theta}{412,560} & \frac{g \text{ t K} \sin 2\theta}{412,560} \\ \frac{T \text{ t K} \sin 2\theta}{412,560} & \frac{T \text{ t K} \sin 2\theta}{412,560} & 0 \end{bmatrix} \begin{bmatrix} A_{vx}^{2} \\ A_{vz}^{2} \end{bmatrix}$$

The significance of the individual errors with respect to the system error can be seen by considering an example. Assume a missile flight trajectory of 50 nautical miles having a 10 g, 10-second boost period, and a total flight time of 200 seconds. The IMU components selected provide an accuracy of 1 mile circular error probability (that is, there is a 50% probability of each missile falling within a circle about the target having a radius of 300 feet). The contribution to the system error is shown in Figure 16 as function of the amplitude of the sinusoidal vibration. It can be seen that at the 3 g level the error contributions start becoming appreciable, especially those which are a function of the square of vibration. However, the total summation of the individual errors is dependent upon the polarity of each of the errors. Since the polarity is defined by the specific physical condition of each of the instruments, either a positive or negative direction can result. Hence some cancellation of the errors can occur.

Summarizing the individual results, the system error equation can be written as follows

$$S_{\varepsilon} = A_{V} + A_{N} + A_{S} + G_{\varepsilon}$$

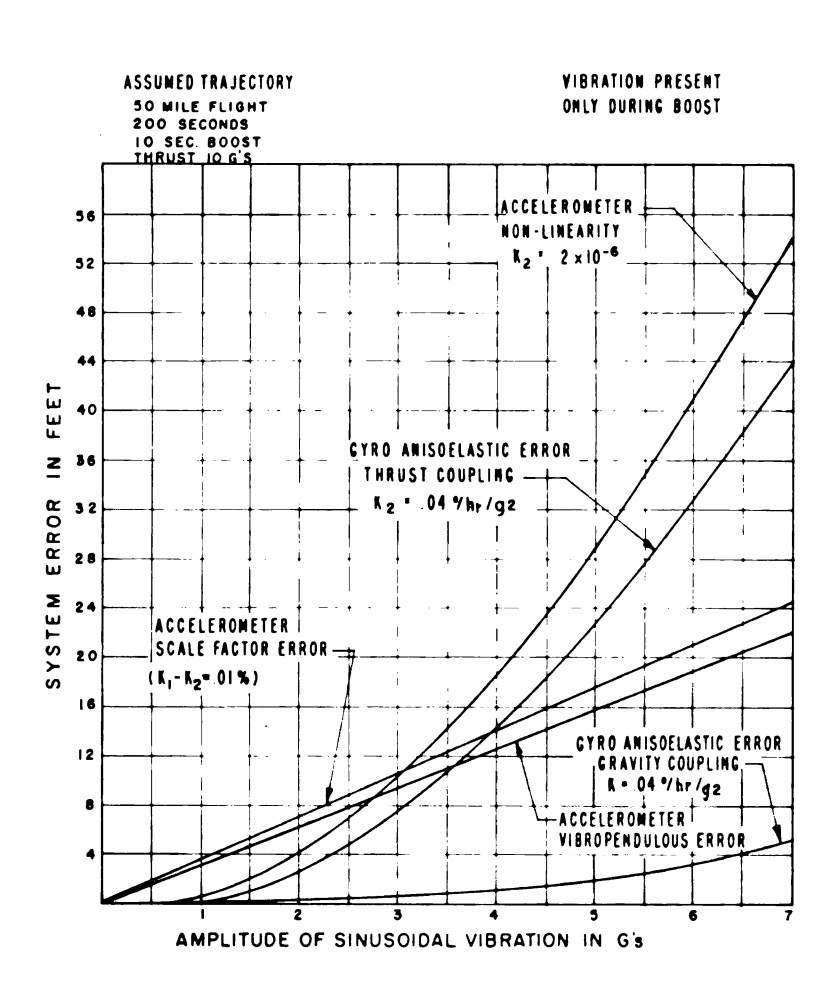


FIGURE 16

CONTRIBUTION TO SYSTEM ERROR BY PLATFORM INSTRUMENTS DUE TO SINUSOIDAL VIBRATION

where

 S_{c} = system error, ft.

 A_V = accelerometer vibropendulous error, ft.

 A_{N} = accelerometer nonlinearity error, ft.

 A_{c} = accelerometer scale factor error, ft.

 G_{c} = accelerometer error due to gyro drift, ft.

This expression assumes that the acceleration and velocity errors defined by the individual error equations are appropriately integrated over the time of flight of the missle.

This completes the analyses associated with sinusoidal vibration. The next two sections are concerned with random vibration.

8.0 EFFECT OF RANDOM VIBRATION ON PLATFORM INSTRUMENTS

Whereas sinusoidal vibrations can be described over all time by a particular function, a random vibration can only be defined on the basis of probability. This section will consider random vibration and its effect on accelerometers and gyros.

8.1 ACCELEROMETERS

Three possible sources of error in an accelerometer produced by a random vibration -- and known as vibropendulous torque, non-linearity, and scale factor variation -- will be presented here.

The type of accelerometer to be considered is the pulse-rebalance accelerometer described in Section 6.1.

8.1.1 Vibropendulous Error

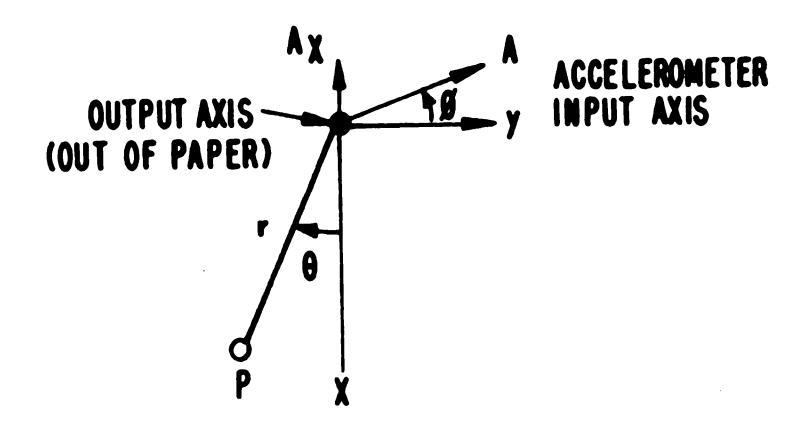
Within the trigger levels of a pulse-rebalance accelerometer (refer to Section 6.1) the pendulum is essentially free with the only restraining force being produced by the damping fluid and the inertia of the pendulum. The vibropendulous error produced by a random vibration acting on such an accelerometer will be developed here.

Consider a pendulum as illustrated in the figure. An applied acceleration (A) is shown along a line at an angle ϕ with the

accelerometer input axis. The components of the applied acceleration are seen to be

$$A_{x} = A \sin \phi = x$$

$$A_y = A \cos \phi = y$$



Each of the components of acceleration will produce a reaction torque due to the pendulosity of the accelerometer. The pendulosity is P = mr where m is the mass of the pendulum and r is the length. Then, the equation of motion is

- P y(t) cos
$$\theta$$
 + P x(t) sin θ = I θ + C θ

Since θ is small, then $\cos \theta$ can be replaced by 1 and $\sin \theta$ = θ , so

-
$$P \ddot{y}(t) + P \ddot{x}(t) \theta = I \theta + C \theta$$

This is a nonlinear equation which can be linearized by considering the magnitude of θ . The maximum value of θ in a pulse-rebalance

accelerometer is 2×10^{-4} radians. Therefore the contribution by the P $\ddot{x}(t)$ θ term is small compared to the P $\ddot{y}(t)$ term and may be disregarded without any significant loss. Then the expression becomes:

$$- P \dot{y}(t) = I \dot{\theta} + C \dot{\theta}$$

Taking the Laplace transform (assuming all the initial conditions are zero) yields

-
$$P\ddot{Y}(s)$$
 = $Is^2 \theta + Cs \theta$

Solving for θ gives

$$\theta(s) = \frac{-\frac{P}{C} \ddot{Y}(s)}{s \frac{I}{C} s + 1}$$

The time solution can be obtained using

$$\theta(t) = -\frac{p}{C} \int_{0}^{t} f_{1}(\tau) f_{2}(t-\tau) d\tau$$

Let

$$-\frac{\tau}{I/C}$$

$$f_1(\tau) = 1 - e$$

$$\mathbf{f_2}(\mathbf{t}-\tau) = \ddot{\mathbf{y}}(\mathbf{t}-\tau)$$

then

$$\theta(t) = -\frac{P}{C} \int_{0}^{t} \left[\frac{u}{y(t-\tau)} - \frac{\tau}{y(t-\tau)} e^{-\frac{\tau}{1/C}} \right] d\tau$$

or

$$\theta(t) = -\frac{P}{C} \int_{0}^{t} \ddot{y}(t-\tau) d\tau$$

$$+ \frac{P}{C} \int_{0}^{t} \ddot{y}(t-\tau)e^{-\frac{\tau}{I/C}} d\tau$$

Since the applied vibration is considered to be wide-sense ergodic, then the first term integrates to zero or

$$\theta(t) = \frac{P}{C} \int_{0}^{t} \frac{-\frac{\tau}{I/C}}{y(t-\tau)e} d\tau$$

As pointed out in Section 6.1 the vibropendulous torque is the product of pendulosity, the cross-axis acceleration (in this case x(t)), and the swing of the pendulum. Therefore the vibropendulous torque is given by

$$M(t) = P \ddot{x}(t) \theta(t)$$

Substituting from above yields

$$M(t) = \frac{P^2}{C} \begin{cases} t & -\frac{\tau}{I/C} \\ \ddot{x}(t) \ddot{y}(t-\tau)e & d\tau \end{cases}$$

Since

$$\ddot{x}(t) = A(t) \sin \phi$$

$$y(t) = A(t) \cos \phi$$

and since the autocorrelation function of

$$A(t)$$
 is $R_{AA}(\tau) = E[A(t) A(t-\tau)]$

the expected torque can be written as

$$M_{E}(t) = E[M(t)] = \frac{P^{2} \sin \phi \cos \phi}{C} \int_{0}^{t} R_{AA}(\tau)e^{-\frac{\tau}{I/C}} d\tau$$

Since the average value of the expected torque is desired, where

$$M_{avg} = \lim_{T \to \infty} \frac{1}{T} \int_{0}^{t} M_{E}(t) dt$$

then

$$M_{\text{avg}} = \frac{P^2 \sin \phi \cos \phi}{C} \quad \lim_{T \to \infty} \int_{0}^{T} \int_{0}^{t} R_{AA}(\tau) e^{-\frac{\tau}{I/C}} d\tau dt$$

Interchanging the order of integration and carrying out the inside integration results in two terms; one reduces to zero with the

substitution for $R_{\mbox{AA}}(\tau)$ as noted below. Considering only the remaining term, gives

$$M_{\text{avg}} = \frac{P^2 \sin \phi \cos \phi}{C} \int_{0}^{\infty} R_{AA}(\tau) e^{-\frac{\tau}{I/C}} d\tau$$

If it is assumed that the input vibration has a constant power spectrum over the bandwidth ω_1 to ω_2 and zero elsewhere, the autocorrelation function can be found to be

$$R(\tau) = \frac{A_0}{\tau} \left(\sin \omega_2 \tau - \sin \omega_1 \tau \right)$$

Substituting into the above yields

$$M_{\text{avg}} = \frac{P^2 A_0 \sin \phi \cos \phi}{C} \int_0^{\infty} \left(\frac{\sin \omega_2 \tau - \sin \omega_1 \tau}{\tau} \right) e^{-\frac{\tau}{I/C}} d\tau$$

or

$$M_{avg} = \frac{P^2 A_0 \sin \phi \cos \phi}{C} \left[\int_0^{\infty} \frac{\sin \omega_2 \tau e^{-\frac{\tau}{I/C}}}{\tau} d\tau - \int_0^{\infty} \frac{\sin \omega_1 \tau e^{-\frac{\tau}{I/C}}}{\tau} d\tau \right]$$

Let

$$\phi_1 = \int_{0}^{\infty} \frac{-\frac{\tau}{I/C}}{\tau} \sin \omega_1 \tau d\tau$$

Differentiating under the integral sign gives

$$\frac{\partial \phi_1}{\partial \omega_1} = \int_0^\infty e^{-\frac{\tau}{I/C}} \cos \omega_1 \tau d\tau$$

or

$$\frac{d \phi_1}{d \omega_1} = \frac{\frac{1}{I/C}}{\left(\frac{1}{I/C}\right)^2 + \omega_1^2}$$

Since

$$\omega_{c} = \frac{1}{I/C}$$

the above becomes

$$\frac{d \phi_1}{d \omega_1} = \frac{\omega_c}{\omega_c^2 + \omega_1^2}$$

Then

$$\phi_1 = \left[\frac{\omega_c}{\omega_c^2 + \omega_1^2} \right] d\omega_1$$

Carrying out the integration gives

$$\phi_1 = \tan^{-1} \left(\frac{\omega_1}{\omega_c} \right)$$

Performing the same type of operation on ϕ_2 gives

$$\phi_2 = \tan^{-1} \left(\frac{\omega_2}{\omega_c} \right)$$

From above it was found that

$$M_{avg} = \frac{P^2 A_0 \sin \phi \cos \phi}{C} (\phi_2 - \phi_1)$$

or

$$M_{avg} = \frac{P^2 A_0 \sin \phi \cos \phi}{C} \left[\tan^{-1} \frac{\omega_2}{\omega_c} - \tan^{-1} \left(\frac{\omega_1}{\omega_c} \right) \right]$$

Since A_0 is in g^2/cps this needs to be corrected to rad/sec or

$$M_{avg} = \frac{P^2 A_0 \sin \phi \cos \phi}{2\pi C} \left[\tan^{-1} \frac{\omega_2}{\omega_c} - \tan^{-1} \frac{\omega_1}{\omega_c} \right]$$

where

 M_{avg} = average vibropendulous torque, dyne-cm

P = pendulosity, gm-cm

 A_0 = power spectral density, g^2/cps

C = damping coefficient, dyne-cm-sec

 ϕ = angle the axis of applied vibration makes with the accelerometer input axis

 ω_1 = lower frequency of vibration input, rad/sec

 ω_2 = upper frequency of vibration input, rad/sec

= accelerometer corner frequency, rad/sec

It can be seen that the vibropendulous torque is a function of the square of the pendulosity, the power spectral density of the applied vibration, the direction of the applied vibration and the relationship of the accelerometer corner frequency to the range of frequencies of the applied vibration.

8.1.2 Nonlinearities

As noted previously the output of an accelerometer can be described as follows:

$$V = K_0 + K_1 A + K_2 A^2 + K_3 A^3 + \cdots$$

where

V = accelerometer output in volts

 $K_0 = bias term$

 K_1 = scale factor

 K_2 = coefficient of second order nonlinearity

 K_3 = coefficient of third order nonlinearity

To determine the effect of random vibration on the output of the accelerometer a simplified approach may be taken¹⁰, It is a reasonable assumption that the random vibration can be described by a finite number of discrete frequency components consisting of a series of sinusoidal vibrations having constant amplitudes, and random phase relationships such that the rms value over any reasonable time period remains constant.

Let all the vibration in a strip $\Delta\omega$ be represented by a single discrete frequency. Let the magnitude of this discrete component be N. Since the assumed vibration is assumed to range from 0 to an

upper frequency of G then there will be $G/\Delta\omega$ discrete components. The approximation for the vibration can then be written

$$A(t) = \sum_{n=1}^{G/\Delta\omega} n \sin (n \Delta\omega t + \phi)$$

where

 ϕ = random phase angle

As $\Delta\omega \to 0$ this approximation becomes very good. For use here let $\Delta\omega = 1$ which results in the approximation for the vibration as

$$A(t) = \sum_{n=1}^{G} n \sin (n t + \phi)$$

Considering only the second order nonlinearity and making the substitution into the above expression for the output of the accelerometer results in the term

$$K_{2} \begin{pmatrix} G \\ \sum_{n=1}^{\infty} N \sin (n t + \phi) \end{pmatrix}^{2}$$

Carrying out the multiplication results in terms of the form

$$K_2 N^2 \sin^2 (nt + \phi_1) + K_2 N^2 \sin (nt + \phi_n) \sin (mt + \phi_m)$$

The rms value is

$$A_{rms} = \sqrt{\frac{N^2G}{2}}$$

Therefore, the error in terms of the rms value is

$$V = K_2 A_{rms}^2$$

where

Thus, with the rectification effect of the accelerometer, each frequency contributes to the error. In addition, the error is also related to the bandwidth of the accelerometer which certainly is reasonable since frequencies above the bandwidth of the accelerometer would not be expected to add to the error. From this consideration, it can be seen that two ways of minimizing the error are by reduction in the error coefficient and decreasing the accelerometer bandwidth.

8.1.3 Scale Factor Error

As with sinusoidal vibration, a difference in the scale factor over the positive and negative range of operation of a pulse-rebalance accelerometer produces an error when subjected to random vibration. This section derives the error equation for such a condition. Here, again, the random vibration is assumed to be widesense ergodic.

Consider the input vibration applied to the accelerometer as shown in Figure 17. The vibration is assumed to have a normal distribution with a zero mean. For an ideal accelerometer the scale factor is a constant over the range of operation. Therefore, for a given input, the output would also be a normal distribution having a zero mean. In this case there is no error introduced by the accelerometer.

Now consider the non-ideal condition where the scale factor is different for the positive and negative regions. With the given input the output amplitudes can be found to be

$$Z = y G(y) = \begin{cases} y \text{ for } -\infty \leq y \leq 0 \\ ky \text{ for } 0 \leq y \leq \infty \end{cases}$$

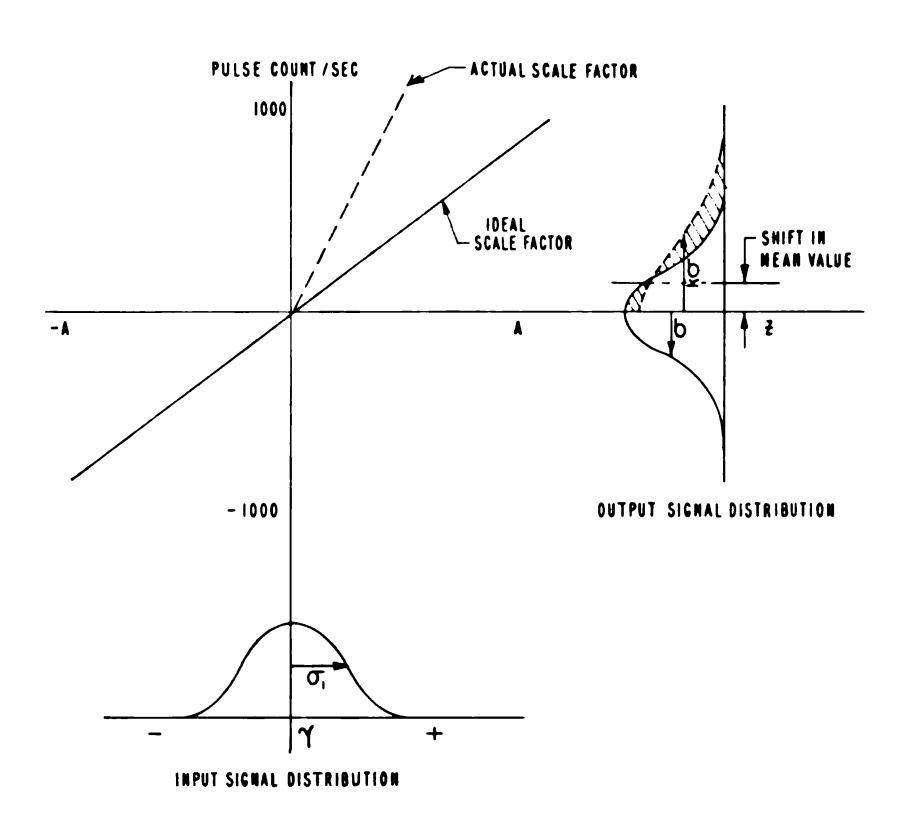


FIGURE 17

SCALE FACTOR ERROR ON SIGNAL DISTRIBUTION

where

Z = output amplitude

y = input amplitude

G(y) = transfer characteristics of the

accelerometer (scale factor)

k = ratio of non-ideal to ideal scale factors

The output probability density function, $\mathbf{p}_{o}(\mathbf{y})$, would then be

$$p_{i}(y) = \begin{cases} p_{i}(y) & \text{for } -\infty \leq y \leq 0 \\ \frac{1}{k} p_{i}(y) & \text{for } 0 \leq y \leq \infty \end{cases}$$

and must have a value such that

$$\int_{-\infty}^{\infty} p_{0}(y) dy = 1 = \int_{-\infty}^{0} p_{i}(y) dy + \frac{1}{k} \int_{0}^{\infty} p_{i}\left(\frac{y}{k}\right) dy$$

The input probability density function can be seen to be

$$p_{i}(y) = \frac{1}{\sigma \sqrt{2\pi}} e^{-\frac{y^2}{2\sigma^2}}$$

The probability density function associated with the non-ideal condition can be found to be

$$\frac{1}{k} p_i \left(\frac{y}{k} \right) = \frac{1}{k \sigma \sqrt{2\pi}} e^{-\frac{y^2}{2k^2 \sigma^2}}$$

It is desired to determine the effect on the mean of the output. The mean value, \bar{y} , is equal to the first moment of the density function. Then

$$\bar{y}_1 = \int_{-\infty}^{0} y \, p_{\hat{1}}(y) \, dy = \frac{1}{\sigma \sqrt{2\pi}} \int_{-\infty}^{0} y \, e^{-\frac{y^2}{2\sigma^2}} \, dy = -\frac{\sigma}{\sqrt{2\pi}}$$

and

$$\bar{y}_2 = \frac{1}{k} \int_0^\infty y \, p_i \left(\frac{y}{k}\right) = \frac{1}{k \, \sigma \sqrt{2\pi}} \int_0^\infty y \, e^{-\frac{y^2}{2k^2 \, \sigma^2}} \, dy = \frac{k\sigma}{\sqrt{2\pi}}$$

Since the mean is equal to the sum of the individual means, then

$$\bar{y} = \bar{y}_1 + \bar{y}_2 = \frac{\sigma}{\sqrt{2\pi}} (k-1)$$

Thus it can be seen that the non-ideal condition results in a shift in the mean to some non-zero value. Since the expression for the output of a pulse-rebalance accelerometer is

$$P = K At$$

where

P = accelerometer output, pulses

K = scale factor, pulses/sec/g

A = acceleration input, g's

g = gravity

t = time in sec

the error due to the random vibration can be found to be

$$P_E = \frac{\sigma}{\sqrt{2\pi}}$$
 (k-1) Kt

The resulting velocity error is

$$V_{E} = \sum_{i=1}^{N} \frac{\sigma}{\sqrt{2\pi}} \quad (k-1) \quad Kt_{i}$$

where

 σ = rms value of random vibration

N = number of seconds

Hence, the importance of maintaining the scale factor to a constant value has been shown.

8.2 GYROS

The gyro drift errors due to mass unbalance and anisoelastic effects caused by random vibration will be considered in this section.

8.2.1 Mass Unbalance Drift

As already shown for sinusoidal vibrations, no error is produced by random vibrations due to gyro mass unbalance. This may be readily shown by considering the expression for drift error due to mass unbalance:

$$\dot{\phi} = \frac{K_1}{T} \int_{0}^{T} A dt$$

where

 $\dot{\phi}$ = drift rate in deg/hr

K₁ = error coefficient due to mass
unbalance, deg/hr/g

A = total acceleration, g's

If the input acceleration is presumed to consist of a random vibration having a zero mean, the integral is equivalent to zero and consequently no drift error is contributed by the mass unbalance term. This may be further verified by again referring to the transfer function for the gyro as:

$$\frac{\rho}{T} = \frac{1/D}{s (\tau s + 1)}$$

where

$$\tau$$
 = time constant I/D

If the input torque is assumed to be a wide-sense ergodic random process and the input power spectral density is represented by $S_T(\omega)$, then the output power spectral density is represented by

$$S_{\rho}(\omega) = \left| H(j\omega) \right|^2 S_{T}(\omega)$$

where

H
$$(j\omega)$$
 = complex frequency response

Since the overall magnitude of H $(j\omega)$ is less than one, the output power spectral density will be small with respect to one. Therefore the motion of the mass unbalance due to the random vibration will be small and in turn the vibropendulous error will be insignificant.

8.2.2 Anisoelastic Drift

A gyro has elastic deflections that take place under vibration. Since the metal used in the fabrication of the gyro is not perfect, variations in the deflections occur producing anisoelastic torque. The literature⁸ has already treated such a condition under random vibration and the pertient equations will be presented here.

The mean torque about the gyro output axis due to random vibration is given by

$$\bar{T}_{OA} = \frac{(980)^2 \text{ m sin } 2\theta}{2} \int_{0}^{\infty} \phi_{AA}(f) \left[R_e K_2 (jf) - R_e K_1 (jf) \right] df$$

where

TOA = average anisoelastic torque about the gyro OA (output axis) due to random vibration, dyne-cm

m = mass of gyro rotor, grams

e angle between the line of applied vibration and the gyro spin reference axis

φ_{AA}(f) = power spectral density of applied vibration acceleration transmitted to gyro case, G²/cps

$$R_{e} K_{i} (jf) = \frac{1}{4\pi^{2}} \left(\frac{f_{n_{i}}^{2} - f^{2}}{\left(\frac{f_{n_{i}}^{2} - f^{2}}{n_{i}} \right)^{2} + 4\zeta_{i}^{2} f_{n_{i}}^{2}} \right)$$

with

 f_{n_1} , f_{n_2} = undamped natural frequencies of rotor elasticity along the SRA and IA respectively, cps

 ζ_i = damping ratio

SRA = spin reference axis

IA = input axis

From the above expression for the mean torque it can be seen that if the elastic characteristics along the spin reference axis and the input axis of the gyro are identical, the average torque is zero. However, if a difference exists then a mean torque is developed which is a function of the power spectral density, the mass of the rotor and the direction of applied vibration.

The drift due to the anisoelastic effects can be found through the use of the gyro equation

$$\omega = \frac{\bar{T}_{OA}}{H}$$

where

 ω = gyro drift, rad/sec

 \bar{T}_{OA} = mean anisoelastic torque, dyne-cm

H = gyro angular momentum, gm-cm²/sec

This, together with the previous expression for mean torque, provides a means of determining the anisoelastic drift of a gyro due to random vibration.

9.0 SYSTEM ERROR DUE TO RANDOM VIBRATION

In considering the system error due to random vibration, the same system model applies here as already presented in Section 7.0.

Based on this the system error equation - consisting of the error contributions from the gimbal structure, accelerometers, and gyros - is presented.

Assuming a vibration on the case of the IMU, the gimbal structure serves to shape the environment for the accelerometers and gyros. The state model was developed in Section 4.0 with an example given in Section 5.0 and will not be repeated here. Standard approaches applicable to random vibration can be used to find the vibration at the stable element.

For random vibration, also, it was shown that an accelerometer had three types of errors - vibropendulous error, nonlinearity, and scale factor error. From Section 8.1 the vibropendulous error equation was found to be

$$\begin{bmatrix} A_{x} \\ A_{y} \\ A_{z} \end{bmatrix} = \begin{bmatrix} A_{x} & 0 & 0 \\ 0 & A_{y} & 0 \\ 0 & 0 & A_{z} \end{bmatrix} \begin{bmatrix} A_{ox} \\ A_{oy} \\ A_{oz} \end{bmatrix}$$

where

 A_x , A_y , A_y are acceleration errors along the X, Y, Z axes,

 ${\rm A}_{\rm ox},~{\rm A}_{\rm oy},~{\rm A}_{\rm oz}$ are the power spectral density level in the X, Y, Z axes, ${\rm G}^2/{\rm cps}$

and

$$A = \frac{P \sin \phi \cos \phi}{2\pi} \left(\tan^{-1} \frac{\omega_2}{\omega_c} - \tan^{-1} \frac{\omega_1}{\omega_c} \right)$$

where

P = pendulosity, dyne-cm

 ϕ = angle the line of applied vibration makes with accelerometer input axis

 ω_1 = lower frequency limit of applied vibration

 ω_2 = upper frequency limit of applied vibration

 ω_c = accelerometer corner frequency

The error equation for the nonlinearity is

$$\begin{bmatrix} A_{x} \\ A_{y} \\ A_{z} \end{bmatrix} = \begin{bmatrix} \frac{K_{2x}}{K_{1x}} & 0 & 0 \\ 0 & \frac{K_{2y}}{K_{1y}} & 0 \\ 0 & 0 & \frac{K_{2z}}{K_{1z}} \end{bmatrix} \begin{bmatrix} A_{rms}^{2}_{(x)} \\ A_{rms}^{2}_{(y)} \\ A_{z}^{2}_{rms}_{(z)} \end{bmatrix}$$

The equation for scale factor error can be found to be

$$\begin{bmatrix} A_{x} \\ A_{y} \\ A_{z} \end{bmatrix} = \begin{bmatrix} \sum_{i=1}^{N} \frac{1}{\sqrt{2\tau}} (k-1)Kt_{i} & 0 & 0 \\ 0 & \sum_{i=1}^{N} \frac{1}{\sqrt{2\tau}} (k-1)Kt_{i} & 0 \\ 0 & 0 & \sum_{i=1}^{N} \frac{1}{\sqrt{2\tau}} (k-1)Kt_{i} \end{bmatrix} \begin{bmatrix} A_{TBS}_{x} \\ A_{TBS}_{y} \end{bmatrix}$$

As pointed out in Section 7.0, the gyro errors produce a misorientation of the platform such that the accelerometers sense a component of gravity or the thrust vector or the combination of the two. Hence, the accelerometer output is in error by an amount depending upon the gyro drift. The general expressions for the accelerometer error produced by the gyros are

$$A_{X} = g G_{X}$$

$$A_y = g G_y$$

$$A_y = T G_y$$

$$A_z = T G_z$$

where A_x , A_y , A_z are the accelerometer error outputs along the X, Y, Z axes,

g = gravity

T = thrust in g's

and G_x , G_y , and G_z are terms associated with the X, Y, Z axes and are defined as follows:

$$G = \frac{t \, \bar{T}_{oA}}{H}$$

where

t = time in seconds

H = gyro angular momentum, gm-cm²/sec

and

$$\bar{T}_{OA} = \frac{(980)^2 \text{ m sin } 2\theta}{2} \int_{0}^{\infty} \phi_{AA}(f) \left(R_e K_2 (jf) - R_e K_1 (jf) \right) df$$

where

m = mass of gyro rotor, grams

 $\phi_{AA}(f)$ = power spectral density of applied vibration acceleration transmitted to gyro case, g^2/cps

$$R_{e} K_{i} (jf) = \frac{1}{4\pi^{2}} \frac{f_{n_{i}}^{2} - f^{2}}{\left(f_{n_{i}}^{2} - f^{2}\right)^{2} + 4\zeta_{i}^{2} f_{n_{i}}^{2}}, i = 1, 2$$

with

 f_{n_1} , f_{n_2} = undamped natural frequencies of rotor along the spin reference axis and the input axis respectively, cps.

Each of the individual error forms has been developed for the accelerometer and the gyros. It remains to establish the system error due to the combination of errors. In pursuing this, it is reasonable to make the assumption that each of the individual errors has a normal distribution and each is independent of all others.

Then the system error can be found² to be

$$S_{\varepsilon} = \left[A_{V}^{2} + A_{N}^{2} + A_{S}^{2} + G_{\varepsilon}^{2} \right]^{\frac{1}{2}}$$

where

S = system error, ft

 A_V = accelerometer vibropendulous error, ft

 A_N = accelerometer nonlinearity error, ft

 A_{c} = accelerometer scale factor error, ft

 G_{F} = accelerometer error due to the gyros, ft

An example of the errors produced by the platform instruments under random vibration was considered. Here, also, a 50-mile flight was assumed and the results are shown in Figure 18. It can be seen that the contribution to the system error can be significant. The vibration was assumed to have a constant power spectral density over the frequency range from 20 cps to 2000 cps. Therefore, the filtering action of the gimbal structure would tend to reduce the effects as indicated. In all, however, the importance of paying careful attention to vibration has been illustrated.

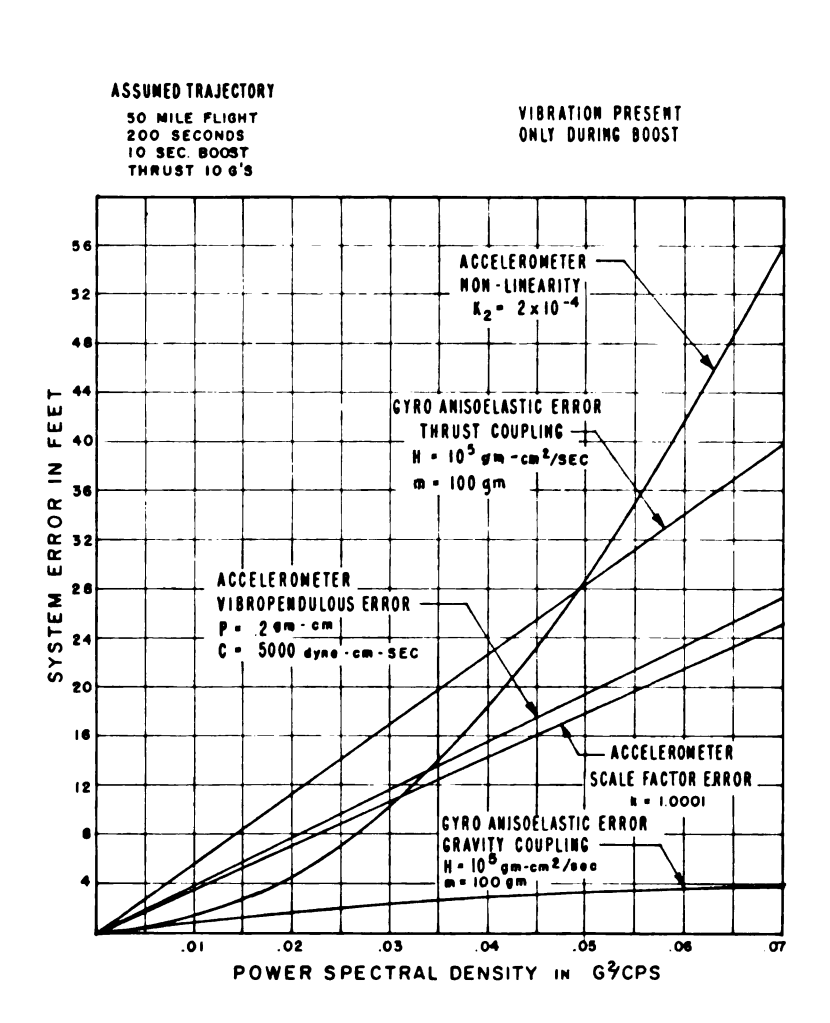


FIGURE 18

CONTRIBUTION TO SYSTEM ERROR BY
PLATFORM INSTRUMENTS DUE TO RANDOM VIBRATION

10.0 CONCLUSIONS

This thesis has presented a unified treatment of the effects of vibration on an IMU from the standpoint of both sinusoidal and random vibration. A state model of the IMU was developed and an example of the application of the state model to the design of an inertial measurement unit was presented. The particular design considerations associated with vibration were indicated. The error equations for vibropendulous torque, nonlinearity, and scale factor variation of the pendulous, pulse-rebalance accelerometer were derived. The error equation was derived for the anisoelastic effects of a gyro under sinusoidal vibration. The system error equation was derived for both the sinusoidal and random vibration effects on an inertial measurement unit. The significance of the vibration effect was pointed out and means for minimizing the effects were indicated. It was shown that the errors due to vibration could range as high as 25% of the allowable miss distance.

REFERENCES

- 1. Aseltine, J.A. "Transform Methods in Linear System Analysis", McGraw-Hill Book Company, Inc., New York, 1958
- 2. Bendat, J.S., "Principles and Applications of Random Noise Theory", John Wiley and Sons, Inc., New York, 1958.
- 3. Bendat, J.S., Enochson, L.D., Klein, G.H., Piersol, A.G.,
 "The Application of Statistics to the Flight Vehicle Vibration
 Problem", ASD-TDR-61-123, Thompson Ramo Wooldridge, Inc., 1961.
- 4. Blackwell, W.A., Koenig, H.E., "Electromechanical System Theory", McGraw-Hill Book Company, Inc., New York, 1961.
- 5. Crandall, S.H., et al., "Random Vibration," Vol. II, The M.I.T. Press, Cambridge, Massachusetts, 1963.
- 6. Fernandez, M., Macomber, G.R., "Inertial Guidance Engineering", Prentice Hall, Inc., Englewood Cliffs, N.J., 1962.
- 7. Hedgepeth, John, Wedmayer, Jr., Edward, "Dynamic and Aeroelastic Problems of Lifting Re-Entry Bodies," Astronautics and Aerospace Engineering, January, 1963.
- 8. Leshnover, Samuel, "Prediction of Anisoelastic and Vibropendulous Effects on Inertial Navigation System Performance in a Linear Random Vibration Environment", National Specialists Meeting on Guidance of Aerospace Vehicles, May 25-27, 1960, Institute of Aeronautical Sciences, pp222-250.
- 9. Pitman, G.R., et al., "Inertial Guidance," John Wiley and Sons, inc., New York, 1962
- Hancock, John C., "An Introduction to the Principles of communication Theory", McGraw-Hill Book Company, Inc., New York, 1961.

